Journal of Medicinal Chemistry

pubs.acs.org/jmc

Article

Discovery of Oral Anticancer 1,2-Bis(hydroxymethyl)benzo[*g*]pyrrolo[2,1-*a*]phthalazine Hybrids That Inhibit Angiogenesis and Induce DNA Cross-Links

Tai-Lin Chen, Anilkumar S. Patel, Vicky Jain, Ramajayam Kuppusamy, Yi-Wen Lin, Ming-Hon Hou, Tsann-Long Su,* and Te-Chang Lee*

Cite This: *J. Med. Chem.* 2021, 64, 12469−12486

Read Online

ACCESS | Metrics & More | Article Recommendations | Supporting Information

ABSTRACT: Designing hybrid molecules with dual functions is one approach to improve the therapeutic efficacy of combination treatment. We have previously conjugated phthalazine and bis(hydroxymethyl)pyrrole pharmacophores to form hybrids bearing antiangiogenesis and DNA interstrand cross-linking activities. To improve the bioavailability, we adopted a benzology approach to design and synthesize a new series of 1,2-bis(hydroxymethyl)benzo[*g*]pyrrolo[2,1-*a*]phthalazines. These new hybrids retained the dual functions and could be formulated into vehicles for intravenous and oral administration. Among them, we demonstrated that compound **19a** with dimethylamine at the C6 position markedly suppressed the tumor growth of human small cell lung cancer cell line H526, squamous lung cancer cell line H520, and renal cancer cell line 786-O in nude mice, implying that compound **19a** is a broad-spectrum anticancer agent. Our results implicated that the conjugation of antiangiogenic and DNA cross-linking is likely to be a helpful approach to improving the efficacy of combination therapy.

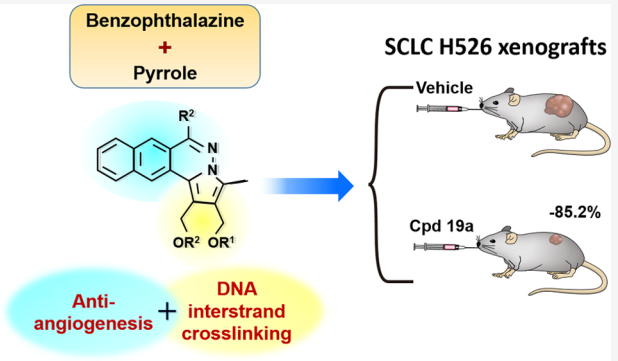

INTRODUCTION

Designing hybrid molecules, which possess multiple modes of action in one molecule, is a promising strategy to discover new chemical entities with marked anticancer activity.[1,2] Since hybrid compounds are designed by conjugating two or more different bioactive moieties, they may possess certain advantages that are features of combination therapy, such as enhancement of efficacy by targeting different pathways in a characteristically synergistic or additive manner, reducing adverse effects, and overcoming drug resistance.[3,4]

Several reviews have reported that pharmacophores such as quinolone, triazole, and indoles are promising moieties for emerging novel hybrid molecules with potential for clinical application.[5−7] During the past several years, we focused on developing antitumor hybrid molecules by coupling a bis(hydroxymethyl)pyrrole moiety (**1**, Figure 1) with other active pharmacophores to generate potent anticancer agents with dual modes of action.[8−13] The scaffold of the bis(hydroxymethyl)pyrrole moiety contains two adjacent hydroxymethyl groups, in which the hydroxyl groups serve as leaving groups, leading to the formation of an electrophilic center at the N-atom of the pyrrole ring. The electrophilic center probably targets DNA and hence induces DNA interstrand cross-links (ICLs).[9,14] Among these hybrids, indolizino[6,7-*b*]indoles (**2**, Figure 1) comprising bis(hydroxylmethyl)pyrrole and *β*-carbolines (**3**, Topo I/II inhibiting moiety) have a broad spectrum of antitumor activity, and in particular, they potently suppressed the tumor growth of non-small-cell lung cancer (NSCLC).[11,12] Furthermore, compound **2a** was shown to have no cross-resistance to vinblastine and gefitinib. Compound **2a**, either alone or in combination with gefitinib (epidermal growth factor receptor (EGFR) inhibitor) or cisplatin (DNA cross-linker), was more potent than irinotecan or cisplatin in suppressing tumor growth in mice bearing NSCLC H460, PC9 (tyrosine kinase inhibitor (TKI)-sensitive NSCLC), and PC9/gef B4 (TKI-resistant NSCLC) xenografts.[11]

The phthalazine scaffold features a nitrogen-containing heterocycle that displays a variety of pharmacological activities.[15] A large number of biologically active compounds containing phthalazine as the pharmacophore have been reported in the literature.[15,16] Many of them were shown to inhibit vascular endothelial growth factor receptor-2 (VEGFR-2) and hence act as antiangiogenic agents.[17−19] More recently, we synthesized a new series of hybrids, namely, 1,2-

Received: October 2, 2020
Published: August 30, 2021

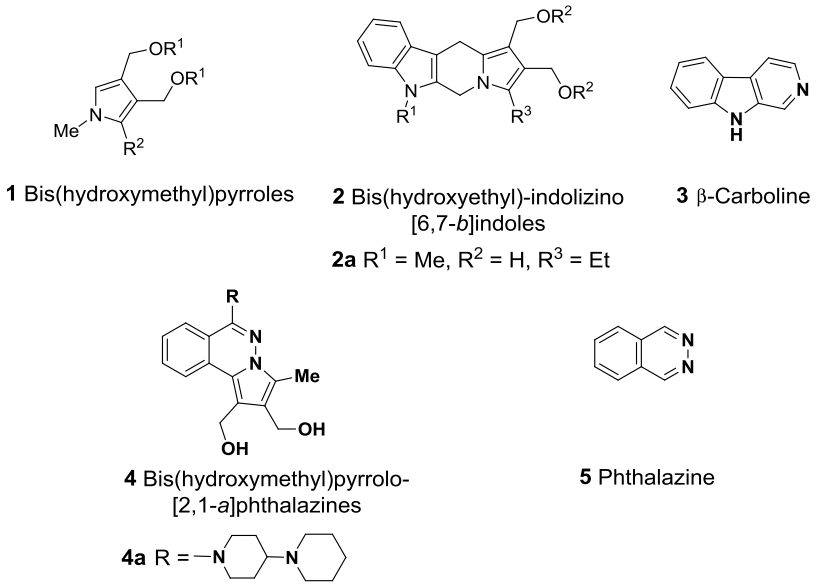

Figure 1. Representative hybrid molecules of bis(hydroxymethyl)pyrrole.

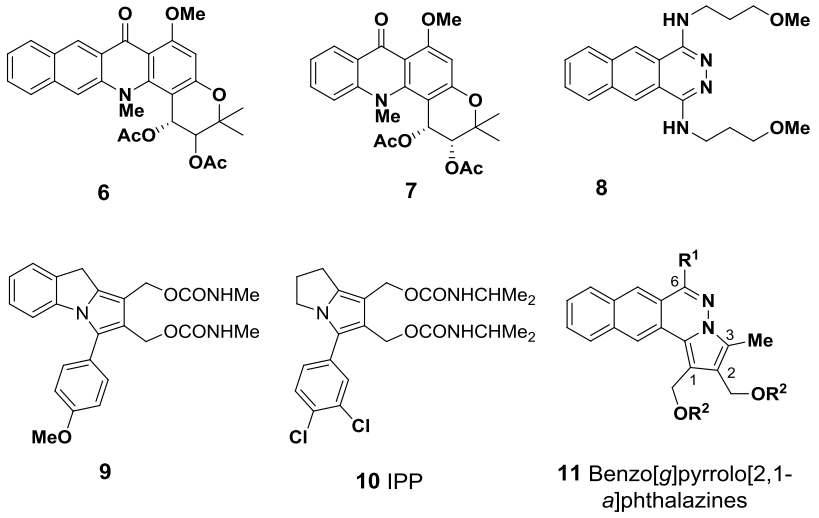

Figure 2. Representative molecules designed by benzology approach.

bis(hydroxymethyl)pyrrolo[2,1-*a*]phthalazines (**4**),[13] which bear a phthalazine pharmacophore (**5**, VEGFR inhibiting group)[19−23] and a bis(hydroxymethyl)pyrrole moiety (**1**, DNA ICL functional group).[24] Of these hybrids, compound **4a** (Figure 1) displayed remarkable biological activity, including strong inhibitory activity against a variety of cancer cell lines, induction of DNA ICLs, interference with cell cycle progression, induction of cell apoptosis in cancer cells, and inhibition of VEGFR-2 in endothelial cells.[13] Furthermore, liposome-encapsulated compound **4d** showed potent antitumor activity in animals.

Structural modification leading to improved chemical stability and pharmacological versatility is an essential medicinal approach to improve the bioavailability of lead compounds.[25−27] Benzology is one of the often used approaches to derive new compounds with improved bioavailability and enhanced biological activity.[28,29] Intriguingly, several reports have revealed the potent biological activities of phthalazine derivatives obtained by benzology. For example, imidazole-based benzo[*g*]phthalazine derivatives were revealed to display potent leishmanicidal activity mediated by the inhibition of Leishmania Fe-superoxide dismutase (SOD) but not human CuZn-SOD.[30,31] For anticancer studies, the synthetic di-*O*-acetyl of (±)-*cis*-1,2-dihydroxy-1,2-dihydroacronycinebenzo[*b*]acronycine (**6**) was more potent than the corresponding di-*O*-acetate of the naturally occurring antitumor (±)-*cis*-1,2-dihydroxyacronycine (**7**) in inhibiting P388 leukemia and colon 38 adenocarcinoma in xenograft models.[32] Several studies have shown the binding of benzo[*g*]phthalazine-based compounds to DNA.[33−35] However, how these phthalazine derivative interact with DNA warrants further investigation. In addition, the heterotricyclic 1,4-bis(alkylamino)benzo[*g*]phthalazine derivative (**8**) was shown to inhibit protein synthesis and to display potent antitumor activity against U-937 human promonocytic leukemia cells in both *in vitro* and *in vivo* models.[36] Nevertheless, we have previously synthesized a series of derivatives of azacyclopenta[*a*]indene (**9**),[8] a benzologue of IPP (**10**),[37] and successfully demonstrated that compound **9**

https://doi.org/10.1021/acs.jmedchem.0c01733
J. Med. Chem. 2021, 64, 12469−12486

Scheme 1. Chemical Synthesis of Bis(hydroxymethyl)benzo[*g*]pyrrolo[2,1-*a*]-phthalazine Derivatives[a]

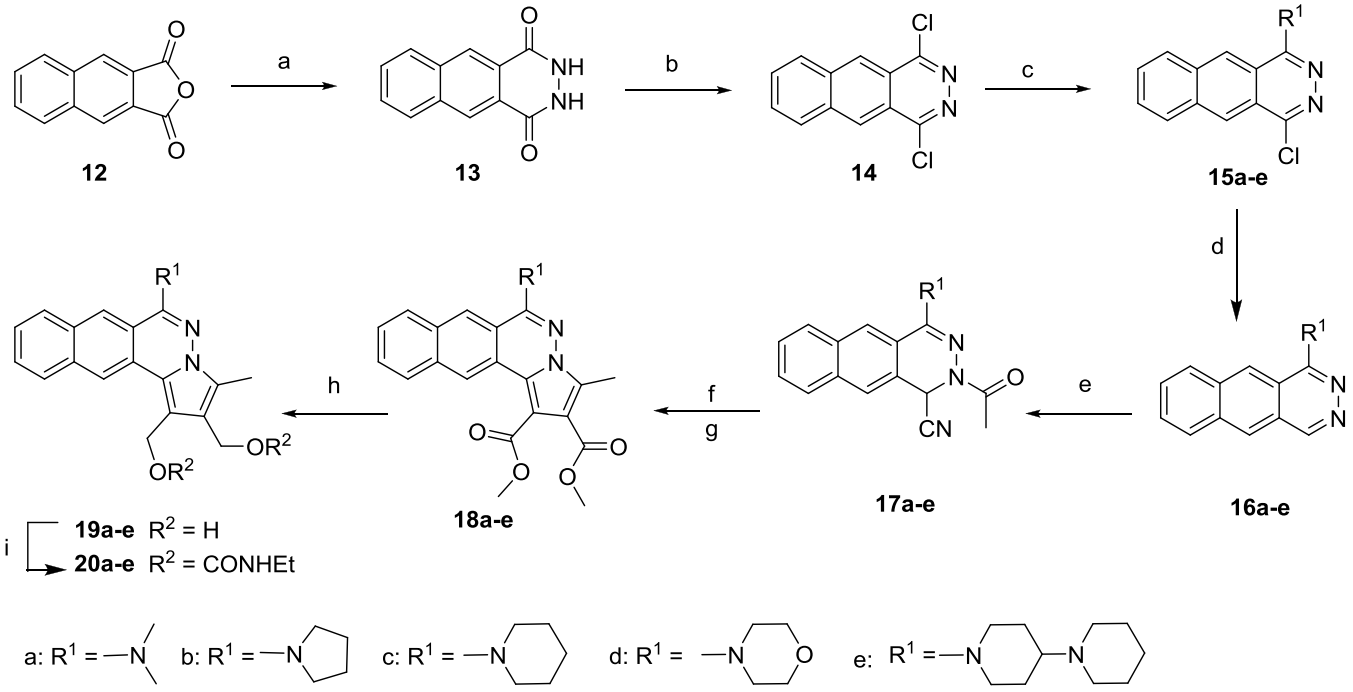

[a]Reagent and condition: (a) hydrazine hydrate/acetic acid, 100 °C; (b) $POCl_3$/pyridine, reflux; (c) R^1NH_2, K_2CO_3, MeCN, reflux; (d) Pd/C, methanol, reflux; (e) TMSCN, $AlCl_3$, MeCOCl, DCM, 27 °C; (f) HBF_4, AcOH, (g) dimethyl acetylenedicarboxylate, DMF, 100 °C; (h) $LiAlH_4$, ether/DCM, 0−30 °C; (i) EtNCO/TEA, 27 °C.

Table 1. Cytotoxicity of Bis(hydroxymethyl)benzo[*g*]pyrrolo[2,1-*a*]phthalazine Derivatives to the Human Lymphoblastic Leukemia Cell Line CCRF and Its Vinblastine-Resistant Subline CCRF-CEM/VBL[a]

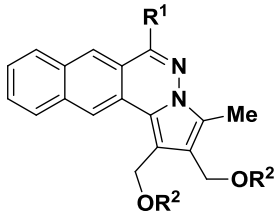

compound	R^1	R^2	CCRF-CEM	CEM/VBL[b]
19a	dimethylamine	H	0.19 ± 0.01	0.10 ± 0.01 [0.53×]
19b	pyrrolidine	H	0.19 ± 0.01	0.14 ± 0.02 [0.74×]
19c	piperidine	H	0.80 ± 0.09	1.01 ± 0.11 [1.26×]
19d	morpholine	H	0.38 ± 0.05	0.56 ± 0.06 [0.74×]
19e	1,4′-bipiperidine	H	0.02 ± 0.01	0.03 ± 0.01 [1.51×]
20a	dimethylamine	CONHEt	0.14 ± 0.01	0.10 ± 0.01 [0.71×]
20b	pyrrolidine	CONHEt	0.42 ± 0.07	0.25 ± 0.06 [0.59×]
20c	piperidine	CONHEt	0.95 ± 0.05	1.20 ± 0.14 [1.26×]
20d	morpholine	CONHEt	0.31 ± 0.02	0.32 ± 0.04 [1.03×]
20e	1,4′-bipiperidine	CONHEt	0.06 ± 0.00	0.10 ± 0.03 [1.82×]
cisplatin			16.53 ± 0.90	8.88 ± 1.86 [0.54×]
vinblastine (nM)			1.41 ± 0.10	392.48 ± 44.75 [278.3×]

[a]The values of IC_{50} (μM) are the average ± SD of at least three experiments using a series of twofold dilutions. [b]The number in brackets is the resistance factor.

exhibited significant *in vitro* cytotoxicity and potent therapeutic efficacy in xenograft models.[8,38]

Since the previously synthesized compound **4a** has poor solubility in common intravenous (i.v.) injection vehicle, the poor solubility could be overcome by encapsulating compound **4a** in liposomes. However, limited amount of compound **4a** in liposome limits remains to be inadequate for its clinical application. To further improve the bioavailability of compound **4**, benzology technique is therefore considered as a helpful approach. In this study, we therefore designed and synthesized a series of benzo[*g*]pyrrolo[2,1-*a*]phthalazines (**11**), which can be considered as benzologues of pyrrolo-[2,1-*a*]phthalazine derivatives.[13] Notably, we discovered compounds with improved bioavailability, including antitumor

https://doi.org/10.1021/acs.jmedchem.0c01733
J. Med. Chem. 2021, 64, 12469−12486

activity, solubility, and oral bioavailability. We describe herein the chemical synthesis and antitumor evaluation *in vitro* and in animal systems (Figure 2).

RESULTS AND DISCUSSION

Chemistry. We have previously demonstrated that the most cytotoxic compound among pyrrolo[2,1-*a*]phthalazines (**4**) bears a Me group at C3.[13] In this study, we synthesized C3-Me-substituted benzo[*g*]pyrrolo[2,1-*a*]phthalazine derivatives with various secondary aliphatic and heterocyclic amines at C6 for structure−activity relationship (SAR) studies. The synthesis of bis(hydroxymethyl)benzo[*g*]pyrrolo[2,1-*a*]-phthalazine derivatives (**19a−e**) and their corresponding bis(ethylcarbamate) congeners (**20a−e**) is shown in Scheme 1. Briefly, the known compound (**13**) was obtained by the reaction of commercially available 2,3-naphthalene dicarboxylic acid anhydride (**12**) with hydrazine hydrate in acetic acid.[35] Treatment of **13** with phosphorus oxychloride in the presence of pyridine afforded 1,4-dichlorobenzo[*g*]phthalazine (**14**).[34] Since the intermediate **14** was unstable and rather hard to be purified, the crude compound **14** was directly used without further purification to react with various secondary amines in the presence of potassium carbonate in acetonitrile and yield compounds **15a−e**. Dechlorination of compounds **15a−e** was performed by reaction with 10% Pd/C in MeOH under H_2 atmosphere to obtain compounds **16a−e**. The reaction of compounds **16a−e** with Me_3SiCN and acetyl chloride in the presence of $AlCl_3$ yielded compounds **17a−e**, which were then converted into hydrofluoroborate salts by treatment with tetrafluoroboric acid-diethyl ether complex in acetic acid, followed by reaction with dimethyl acetylenedicarboxylate (DMAD) to give diesters, compounds **18a−e**. The reduction of diesters **18a−e** by treatment with lithium aluminum hydride (LAH)/ether/dichloromethane (DCM) afforded the corresponding bis(hydroxymethyl) derivatives **19a−e**, which were further converted into their corresponding bis-(ethylcarbamates) congeners (**20a−e**) by treatment with ethyl isocyanate in dimethylformamide (DMF)/triethylamine (TEA) at room temperature. The high-performance liquid chromatography (HPLC) chromatograms, ^1H nuclear magnetic resonance (NMR), ^{13}C NMR, and high-resolution mass spectrometry (HRMS) data of intermediates and new compounds are presented in Figures S1 and S2, respectively.

***In Vitro* Cytotoxicity.** We first evaluated the *in vitro* cytotoxicity of the newly synthesized compounds against the human lymphoblastic leukemia cell line CCRF-CEM for SAR study. As shown in Table 1, bis(hydroxymethyl) derivatives (**19a−e**) are practically as cytotoxic to CCRF-CEM cells as their corresponding bis(ethylcarbamate) derivatives (**20a−e**). Of the compounds examined, compounds **19e** and **20e**, bearing a 1,4′-bipiperidine substituent at C6, are the most cytotoxic. The order of potency against CCRF-CEM is bipiperidine substituent at C6 (**19e**) ≫ dimethylamine (**19a**) ≅ pyrrolidine (**19b**) > morpholine (**19d**) > piperidine (**19c**). This finding is similar to the results for the series of bis(hydroxymethyl)pyrrolo[2,1-*a*]phthalazines (**4**) shown in our previous report.[13] However, the newly synthesized benzo[*g*]pyrrolo[2,1-*a*]phthalazines **19a−e** are indeed more cytotoxic than their corresponding pyrrolo[2,1-*a*]phthalazine derivatives (**4**), confirming the advantage of the benzology approach for generating new leads with improved biological activity. Notably, the newly synthesized compounds are more cytotoxic than cisplatin (Table 1).

Additionally, the CCRF-CEM/VBL cell line, an acquired multidrug-resistant (MDR) cell line featuring P-glycoprotein overexpression and an ∼278-fold resistance to vinblastine, was adopted to define whether the MDR cancer cells were cross-resistant to new hybrids. As shown in Table 1, all tested compounds have little or no cross-resistance to vinblastine. We also confirmed this finding using the other P-glycoprotein overexpressed MDR cells, KB/vin 10 cells, which were derived from KB cells (Table S1).[12] This suggests that all of the new hybrids are not good substrates for membrane MDR transporters (e.g., P-glycoprotein). Thus, we may infer that the newly synthesized compounds are effective against MDR tumors.

Since 1,2-bis(alkylcarbamate) derivatives were not fully stable during storage at 4 °C, the following biological studies were performed using only 1,2-bis(hydroxymethyl)-3-methyl derivatives. We previously demonstrated that pyrrolo[2,1-*a*]phthalazine hybrids exhibited significant cytotoxicity to various lung cancer cells *in vitro*.[13] To understand whether the newly synthesized benzo[*g*]pyrrolo[2,1-*a*]phthalazine hybrids (**19a−e**) have superior antitumor activity to that of pyrrolo[2,1-*a*]phthalazines, we investigated the inhibitory effects of compounds **19a−e** on the inhibition of a panel of lung cancer cells, including 7 NSCLC cell lines (H460, A549, H520, H226, H2170, H1975, and H1650) and 5 SCLC cell lines (H1417, H211, H146, H526, and H82). Among NSCLC cells, H460 and A549 cells were classified as lung large cell carcinoma, H520, H226, and H2170 as lung squamous cell carcinoma, and H1975 and H1650 as lung adenocarcinoma. Among the SCLC cell lines, H1417 and H211 were derived from SCLC tumors, while H146, H526, and H82 were derived from SCLC metastatic sites, bone marrow, or pleural effusion, respectively. As summarized in Table 2, compounds **19a−e** displayed significant cytotoxicity to all lung cancer cell lines tested. The potency against lung cancer cells was similar to that against CCRF-CEM cells and likely dependent on the substituent at C6. The 1,4′-bipiperidine-substituted compound **19e** was generally the most cytotoxic to lung cancer cells. Compounds **19a** and **19b** also displayed significant cytotoxic activity to lung cancer cells. Furthermore, SCLC cells were more susceptible to these new hybrids than NSCLC cells, and H526 cells were the most sensitive cell line. Notably, the new hybrids were more cytotoxic than cisplatin (DNA cross-linking agent), irinotecan (topoisomerase I inhibitor), and sorafenib (protein kinase inhibitor), which are currently used for the treatment of lung cancer patients in the clinic.

Furthermore, we evaluated the cytotoxicity of the new hybrids against other solid tumor cell lines, such as colorectal cancer cell line HCT-116, pancreatic cancer cell line Paca S1, and renal cell carcinoma (RCC) cell line 786-O (Table 3). These new agents were more cytotoxic than current therapeutic agents, such as cisplatin, irinotecan, and sorafenib, to the tested tumor cell lines. Notably, RCC 786-O cells were more susceptible to the tested compounds than HCT-116 and Paca S1 cells. As shown in Table S2, we noticed that so-called normal cells, such as human fetal colon epithelial (FHC) cells and human skin fibroblasts (CRL-1508), were more resistant to compounds **19a** and **19e**.

In summary, the newly synthesized benzologue derivatives clearly exhibited potent cytotoxicity against human lymphoblastic leukemia and various solid tumor cells *in vitro*. In general, compound **19e** (bearing a 1,4′-bipiperidine moiety at C6) was the most cytotoxic, whereas **19c** (bearing a piperidine

https://doi.org/10.1021/acs.jmedchem.0c01733
J. Med. Chem. 2021, 64, 12469−12486

Table 2. Cytotoxicity of Bis(hydroxymethyl)benzo[*g*]pyrrolo[2,1-*a*]phthalazine Derivatives to a Batch of Human NSCLC and SCLC Cells[a]

	NSCLC							SCLC				
compound	H460	A549	H520	H226	H2170	H1975	H1650	H1417	H211	H146	H82	H526
19a	1.02 ± 0.16	1.55 ± 0.27	1.37 ± 0.79	0.67 ± 0.23	3.27 ± 0.88	0.98 ± 0.36	1.20 ± 0.10	0.42 ± 0.19	0.12 ± 0.01	1.17 ± 0.29	0.31 ± 0.14	0.04 ± 0.01
19b	0.78 ± 0.24	2.08 ± 0.19	1.40 ± 0.23	1.03 ± 0.54	2.63 ± 1.61	1.19 ± 0.24	1.57 ± 0.50	0.60 ± 0.34	0.17 ± 0.02	1.01 ± 0.24	0.41 ± 0.15	0.02 ± 0.01
19c	3.03 ± 0.48	5.61 ± 0.54	3.66 ± 0.22	3.12 ± 0.36	7.84 ± 0.44	4.87 ± 0.48	7.70 ± 0.51	1.37 ± 0.03	1.18 ± 0.05	2.65 ± 1.39	1.48 ± 0.66	0.28 ± 0.04
19d	1.18 ± 0.10	1.24 ± 0.01	1.00 ± 0.73	0.85 ± 0.17	1.43 ± 0.41	1.22 ± 0.23	1.42 ± 0.13	0.37 ± 0.01	0.21 ± 0.08	1.02 ± 0.16	0.40 ± 0.16	0.04 ± 0.01
19e	0.92 ± 0.12	0.29 ± 0.02	0.23 ± 0.04	0.14 ± 0.01	0.43 ± 0.09	0.23 ± 0.09	0.39 ± 0.11	0.25 ± 0.05	0.03 ± 0.02	0.20 ± 0.15	0.04 ± 0.01	0.04 ± 0.05
cisplatin	5.11 ± 0.22	11.64 ± 0.73	42.09 ± 2.95	9.77 ± 1.53	27.27 ± 5.65	9.19 ± 1.31	8.60 ± 1.37	40.81 ± 5.97	3.47 ± 0.20	10.20 ± 2.99	1.75 ± 0.39	0.81 ± 0.38
irinotecan	5.15 ± 0.49	19.71 ± 0.71	36.16 ± 10.99	4.25 ± 1.57	18.81 ± 1.79	21.49 ± 5.07	39.67 ± 3.50	9.79 ± 0.84	2.81 ± 0.48	11.51 ± 6.53	2.26 ± 0.01	0.49 ± 0.06
sorafenib	3.68 ± 0.28	10.70 ± 1.57	11.50 ± 0.62	7.92 ± 0.86	22.59 ± 3.20	9.27 ± 0.71	18.09 ± 1.76	5.84 ± 0.18	16.47 ± 1.68	8.01 ± 0.23	1.77 ± 0.12	14.68 ± 0.74

[a]The values of IC_{50} (μM) are the average ± SD of at least three experiments using a series of twofold dilutions.

Table 3. Cytotoxicity of Bis(hydroxymethyl)benzo[*g*]pyrrolo[2,1-*a*]phthalazine Derivatives to Colorectal (HCT-116), Pancreatic (Paca S1), and Renal (786-O) Cancer Cell Lines[a]

compound	HCT-116	Paca S1	786-O
19a	0.65 ± 0.02	3.98 ± 1.04	0.37 ± 0.02
19b	0.93 ± 0.12	1.04 ± 0.08	0.39 ± 0.09
19c	4.13 ± 0.27	10.01 ± 1.64	3.12 ± 0.09
19d	1.13 ± 0.02	0.88 ± 0.26	0.39 ± 0.12
19e	0.24 ± 0.02	0.16 ± 0.03	0.17 ± 0.04
cisplatin	9.17 ± 0.67	27.04 ± 0.98	7.42 ± 0.32
irinotecan	12.03 ± 1.15	14.98 ± 0.78	2.25 ± 1.44
sorafenib	3.68 ± 0.28	4.43 ± 0.11	15.62 ± 0.90

[a]The values of IC_{50} (μM) are the average ± SD of at least three experiments using a series of twofold dilutions.

moiety at C6) was the least cytotoxic among the compounds tested. In addition to compound **19e**, compounds **19a** and **19b** also displayed relatively high potency against SCLC cells. As previously reported, compound **4a** (Figure 1), one of the 1,2-bis(hydroxymethyl)pyrrolo[2,1-*a*]phthalazines with a 1,4′-bipiperidine moiety at C3 (i.e., compound **29** in our previous report),[13] was also the most cytotoxic among its hybrid series. Due to its poor solubility, 1,4′-bipiperidine bis-(hydroxymethyl)pyrrolo[2,1-*a*]phthalazine (**4a**) had to be encapsulated in a liposomal formulation prior to testing its anticancer activity.[13] Fortunately, we found that compound **19a** displayed a desirable solubility in a mixture of Tween 80/PEG 400/Kolliphor HS15/ethanol/5% dextrose for intravenous (i.v.) administration to animals or a mixture of Tween 80/PEG 400/Kolliphor HS40/ethanol/5% dextrose for oral (p.o.) administration. Therefore, compound **19a** was selected as the representative compound for mechanistic study and *in vivo* antitumor activity evaluation.

DNA Interstrand Cross-Linking. As previously mentioned, benzo[*g*]pyrrolo[2,1-*a*]phthalazine hybrids contain a bis(hydroxymethyl)pyrrole moiety (responsible for DNA ICL) and benzophthalazine (responsible for antiangiogenesis). The newly synthesized hybrids were designed to challenge traditional combinational therapies using DNA ICL agents and angiogenic inhibitors. We therefore performed alkaline gel electrophoresis[39] to show the formation of DNA ICLs by compounds **19a**–**e**. As shown in Figure 3A, all of these compounds were able to interact with DNA and form DNA ICLs in a dose-dependent manner. To confirm that these compounds were also able to induce DNA ICLs in cells, SCLC H526 cells were treated with compound **19a** and subjected to a modified comet assay.[8] As shown in Figure 3B, either compound **19a** or cisplatin dose-dependently and significantly induced shortened tail moments in H526 cells that were irradiated with X-rays. Since shorter DNA tails in X-ray-irradiated cells revealed higher levels of DNA ICLs in cells, our results clearly showed DNA ICL induction by the treatment of H526 cells with compound **19a** and cisplatin (Figure 3C). Furthermore, we observed that compound **19a** was able to induce DNA ICLs at a dose range much lower than that of cisplatin.

To determine the drug–DNA interaction by biophysical experiments, we measured the fluorescence emission spectra of compound **19a** in the presence of two DNA duplexes with CG- and TA-rich sequence (Figure 4A) as previously described.[40,41] As shown in Figure 4B, we observed an increase in

https://doi.org/10.1021/acs.jmedchem.0c01733
J. Med. Chem. 2021, 64, 12469–12486

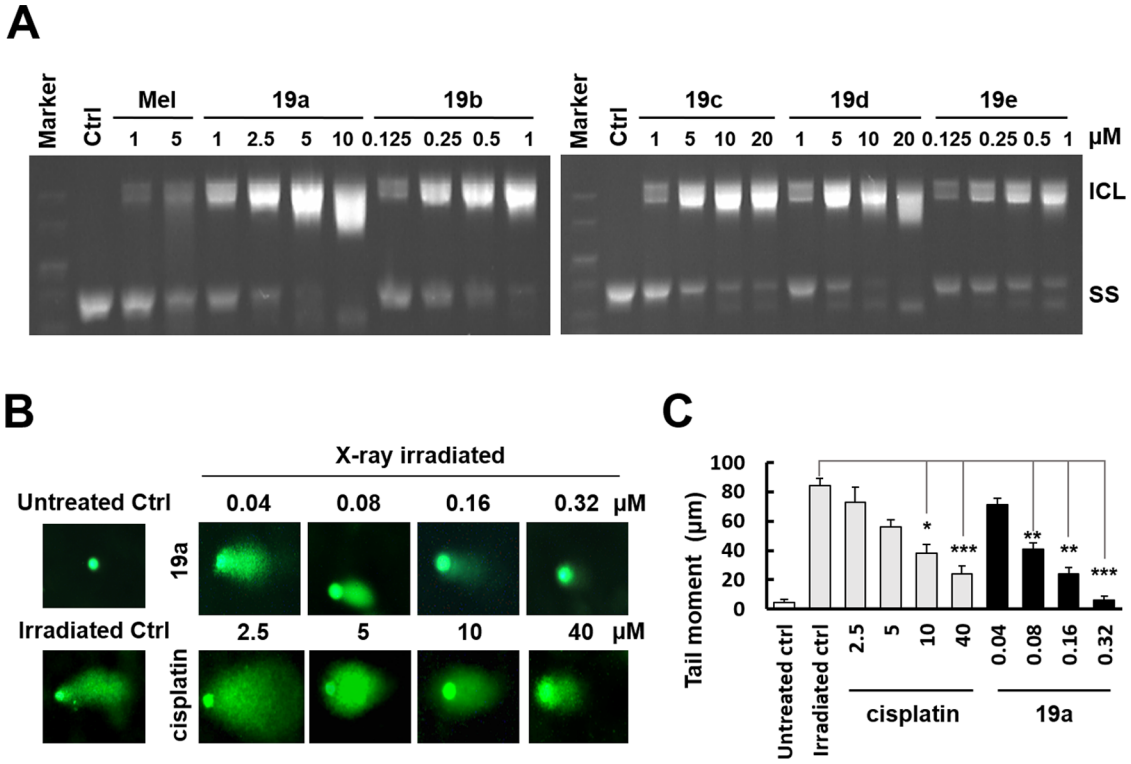

Figure 3. DNA ICLs induced by benzo[*g*]pyrrolo[2,1-*a*]phthalazine hybrids. (A) Alkaline gel electrophoretic analysis. The plasmid pEGFP-N1 DNA was incubated with various concentrations of compounds **19a**–**e** at 37 °C for 2 h. After linearization by digestion with *Bam*H1, the DNA was denatured under alkaline conditions. The interstrand cross-linked (ICL) and single-strand (SS) DNA molecules were electrophoretically separated on alkaline gel. Melphalan (1 and 5 μM) was used as a positive control. (B) Representative images of modified comet assay. SCLC H526 cells were treated with various concentrations of compounds **19a** or cisplatin for 2 h. Afterward, the cells were harvested by trypsinization, irradiated with 20 Gy X-ray, and immediately layered on an agarose gel. Electrophoresis was performed as described in the Experimental Section. Images were taken by a fluorescent microscope. (C) Summarized tail moments of (B). The data were average of three independent experiments. *$p < 0.05$; **$p < 0.01$; and ***$p < 0.001$, compared with cells without treatment by Student's t test.

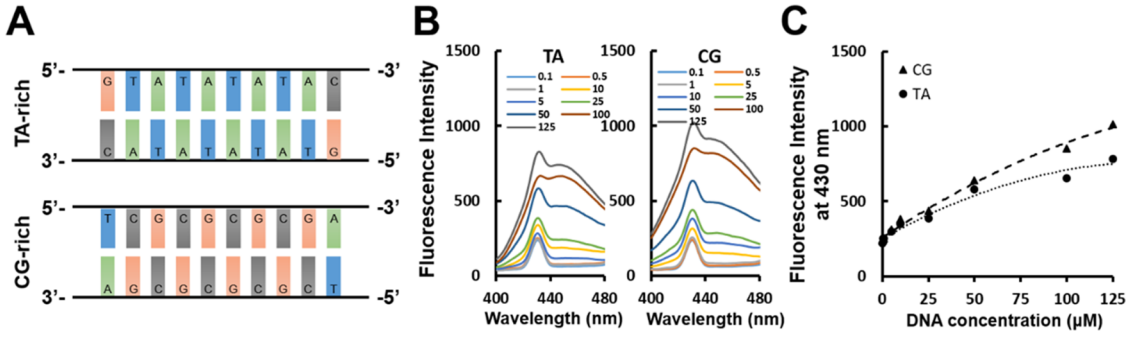

Figure 4. Binding of compound **19a** to DNA duplex. (A) CG-rich and TA-rich DNA duplexes used for binding assay. (B) Enhanced fluorescence emission spectra of compound **19a** (5 μM) in the presence of CG-rich or TA-rich duplexes at different concentrations from 0.1 to 125 μM in sodium cacodylate buffer. The fluorescence emission spectra from 400 to 480 nm were recorded using the excitation wavelength at 380 nm. (C) Binding plot of relative fluorescence intensities of compound **19a** to DNA as described in the Experimental Section. The fluorescence intensity at 430 nm was plotted against DNA concentrations.

fluorescence emission of compound **19a** with DNA duplexes compared to the compound alone control. By plotting the relative fluorescence emission intensity of compound **19a** to various concentrations of DNA duplexes (Figure 4C), the results suggest that compound **19a** preferentially binds to CG-rich DNA than TA–DNA. These findings were consistent with the previous report showing that pyrrole-derived bifunctional can preferentially cross-linked deoxyguanosine residues at DNA duplex with CG sequence.[42] On the other hand, we did not observe the changes in the melting temperature of DNA duplexes in the presence of compound **19a** (Figure S3), implicating that compound **19a** is not a DNA intercalating agent but likely a DNA minor groove binder. Although there is no report showing the inhibitory activity of benzophthalazine derivatives, we also performed the activity assay of topoisomerase I and II.[11] As expected, compounds **19a** and **19b** displayed limited inhibition of topoisomerase I and II at the doses of 100 and 50 μM, respectively (Figure S4). Nevertheless, the binding mechanism of compound **19a** to DNA warrants our further investigation.

https://doi.org/10.1021/acs.jmedchem.0c01733
J. Med. Chem. 2021, 64, 12469–12486

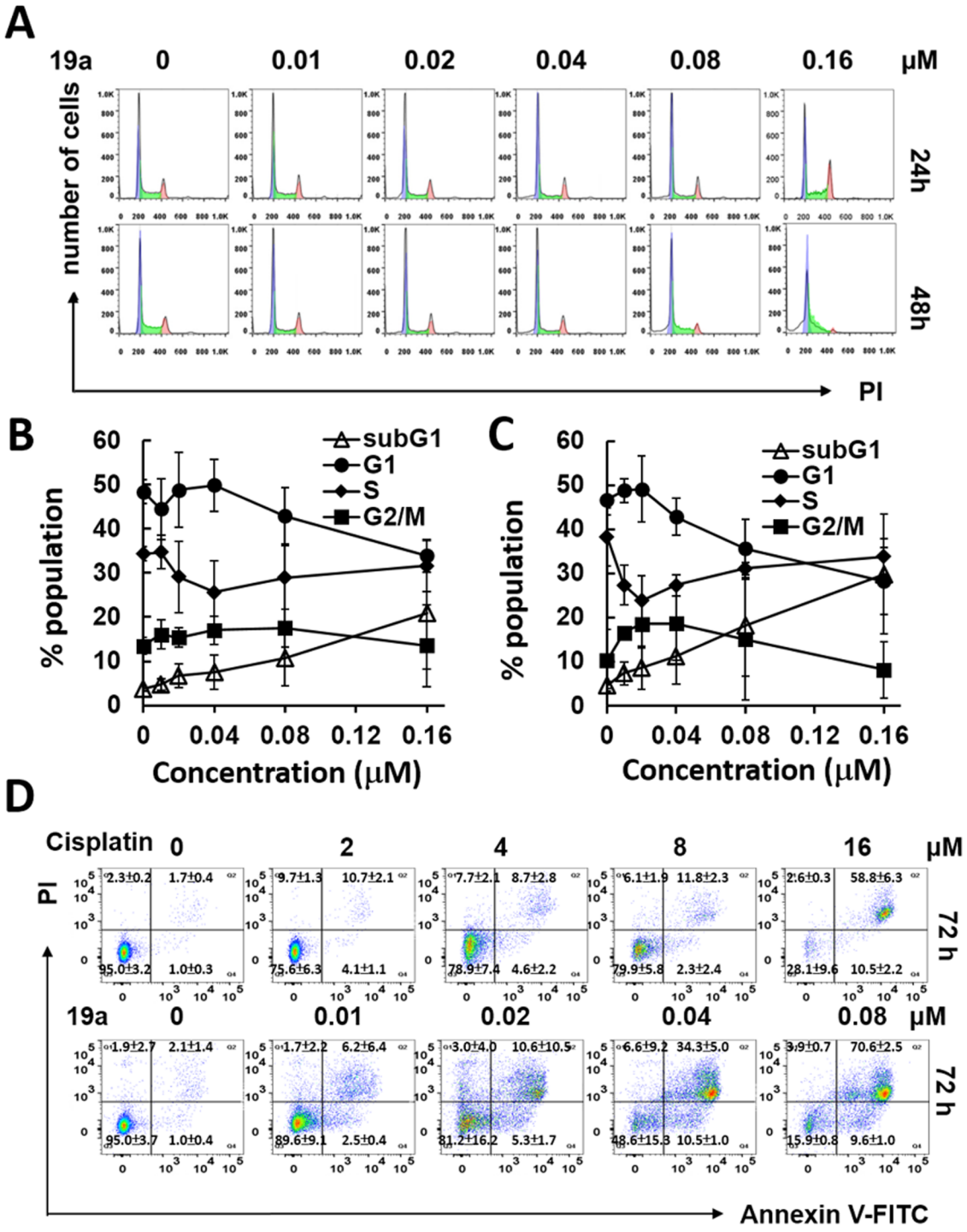

Figure 5. Compound **19a** interferes with cell cycle progression and triggers apoptosis in SCLC H526 cells. (A) Flow cytometric analysis. The logarithmically growing H526 cells were treated with various concentrations of compound **19a** for 24 and 48 h. At the end of treatment, the cell cycle phase was flow cytometrically analyzed. (B, C) Distribution of cell cycle phases. The cell cycle distribution of H526 cells treated with compound **19a** for 24 h (B) and 48 h (C), respectively, was determined using FlowJo 7.6 software. The data were average of three independent experiments. (D) Annexin-V staining assay. The apoptotic death was analyzed using Annexin-V kit. H526 cells were treated with various concentrations of compound **19a** or cisplatin 72 h. At the end of treatment, the cells were harvested, stained with Annexin-V and PI, and subjected flow cytometric analysis.

Cell Cycle Interference and Apoptotic Death. To investigate the effects of compound **19a** on cell cycle progression, H526 cells, a fast-growing cell line, were incubated with compound **19a** at various concentrations for 24 and 48 h and subjected to flow cytometric analysis (Figure 5A). Since the IC_{50} of compound **19a** (72 h treatment) to H526 cells was 0.04 ± 0.01 μM, the dose range used for cell cycle analysis was 0−0.16 μM. As summarized in Figure 5B,C, we observed a decline in S phase cells accompanied by increased G2/M phase cells at a low dose range (<0.08 μM) in H526 cells treated with compound **19a** for 24 and 48 h, respectively. These results suggested that compound **19a** treatment resulted in DNA

https://doi.org/10.1021/acs.jmedchem.0c01733
J. Med. Chem. 2021, 64, 12469−12486

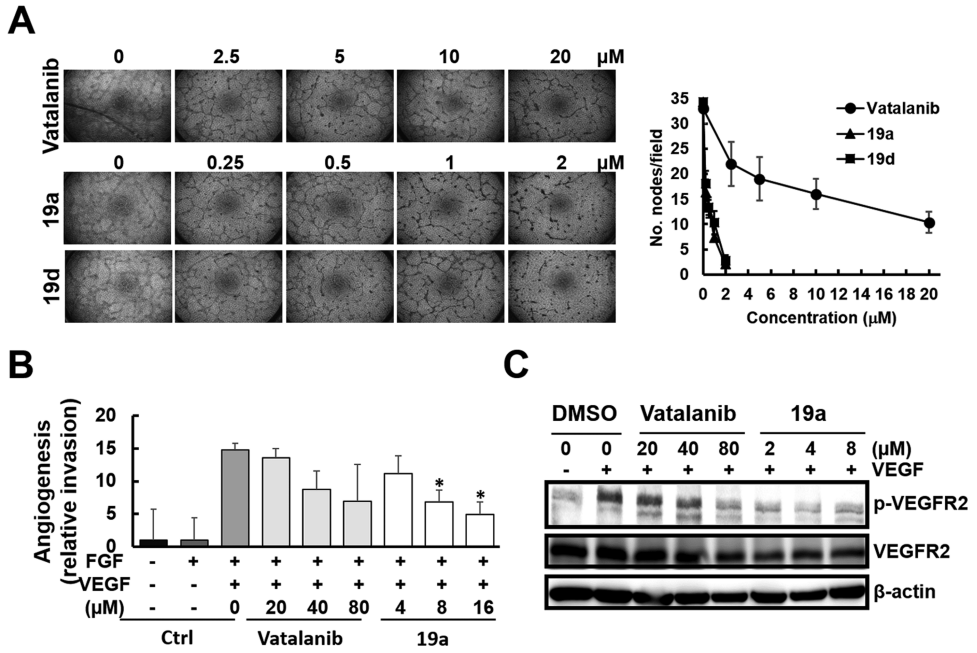

Figure 6. Suppression of angiogenesis by compound **19a**. (A) Tube formation inhibition assay. EA.hy926 cells were cultured on Matrigel-coated plates and treated with various concentrations of **19a** or vatalanib as described in the Experimental Section. Left: representative images of tube formation; right: averaged number of nodes per field. (B) Directed *in vivo* angiogenesis assay (DIVAA). As described in the Experimental Section, angioreactors containing FGF (37.5 ng), EGF (12.5 ng), and various concentrations of compound **19a** and vatalanib were implanted subcutaneously into the abdominal region of mice and allowed infiltration of vessels into angioreactors. Angioreactors without growth factor supplements or only FGF were included as negative control. *$p < 0.05$, compared with cells without treatment by Student's t test. (C) Inhibition of VEGFR-2 phosphorylation. EA.hy926 cells were treated with various concentrations of **19a** and vatalanib for 12 h. At the end of the treatment period, the levels of VEGFR-2 and p-VEGFR were determined by western blot analysis.

damage, suppressing the progression of G2/M phase cells and blocking the progression of G1 phase cells into S phase. Furthermore, upon increasing the concentrations (>0.8 μM), we observed increased subG1 phase cells, an indicator of apoptotic death. We may infer that the severe DNA damage induced by compound **19a** not only abrogated cell cycle progression but also triggered apoptotic death. We further performed an Annexin-V staining assay to confirm apoptotic death induced by compound **19a**. As shown in Figure 5D, treatment of H526 cells with compound **19a** for 72 h indeed induced a dominant population undergoing late apoptosis (upper-right quadrant) in a dose-dependent manner. In addition, compound **19a** was more potent than cisplatin in triggering apoptotic death in H526 cells.

Inhibition of Angiogenesis. Tumor angiogenesis is a mechanism that allows cancer cells to construct new blood vessels and can support tumor growth by providing essential nutrients and oxygen.[43,44] As a result, the development and progression of the tumor and its metastasis are associated with efficient vascular formation.[45] Approximately 30 endogenous proangiogenic factors are known to participate in angiogenesis.[46] Among these factors, vascular endothelial growth factors (VEGFs) play essential roles in angiogenesis.[47] VEGF/VEGFR pathway signaling is required for endothelial cell survival, proliferation, migration, and invasion.[48] The *in vivo* angiogenic response to VEGF in tumors is mainly mediated via the phosphorylated activation of VEGFR-2.[49]

To validate the antiangiogenic properties of the new hybrids, we first determined the cytotoxicity of compounds **19a** and vatalanib against human endothelial EA.hy926 cells. The results showed that compound **19a** was more cytotoxic (IC_{50} = 2.86 ± 1.58 μM) than vatalanib (IC_{50} = 22.32 ± 3.17 μM) to EA.hy926 cells. However, comparison with the IC_{50} values of **19a** against the human SCLC cell lines analyzed showed that compound **19a** was ~6.8- to 71.5-fold less toxic to endothelial EA.hy926 cells. We then compared the antiangiogenic activity of compound **19a** with that of vatalanib by performing a tube formation assay using human endothelial EA.hy926 cells. The results showed that robust tubular structures were formed in the control culture, whereas preincubation with **19a** or vatalanib dose-dependently decreased tube formation (Figure 6A). Conversely, compound **19a** was ~10-fold more potent than vatalanib in suppressing tube formation (Figure 6A right). In addition, with the aid of the directed *in vivo* angiogenesis assay (DIVAA), compound **19a** was ~5-fold more potent than vatalanib in suppressing vascular invasion in an *in vivo* model (Figure 6B). To confirm the antiangiogenic activity of compound **19a**, we performed western blotting analysis. As shown in Figure 6C, compound **19a** significantly suppressed p-VEGFR-2 protein levels, suggesting that **19a** could inhibit VEGFR-2 activation to a similar extent to that achieved by vatalanib. Taken together, our results demonstrated that compound **19a** apparently retained antiangiogenic activity by inhibiting VEGFR-2 activation at a dose range much lower than that of vatalanib.

Therapeutic Efficacy of 19a in Tumor Xenograft Models. Based on the *in vitro* cytotoxicity and solubility, compound **19a** was selected for investigating the therapeutic efficacy in nude mice bearing tumor xenograft models. Mice bearing SCLC H526 tumor cells were i.v. administered a solution of **19a** (20 mg/kg) in a vehicle of Tween 80/PEG 400/Kolliphor HS15/ethanol/5% dextrose (5:5:20:30:40, v/v/v/v/v) via the tail vein for 2 cycles of 5 consecutive days with 1 day of rest (QD × 5 + R) × 2. The efficacy of **19a** was

https://doi.org/10.1021/acs.jmedchem.0c01733
J. Med. Chem. 2021, 64, 12469−12486

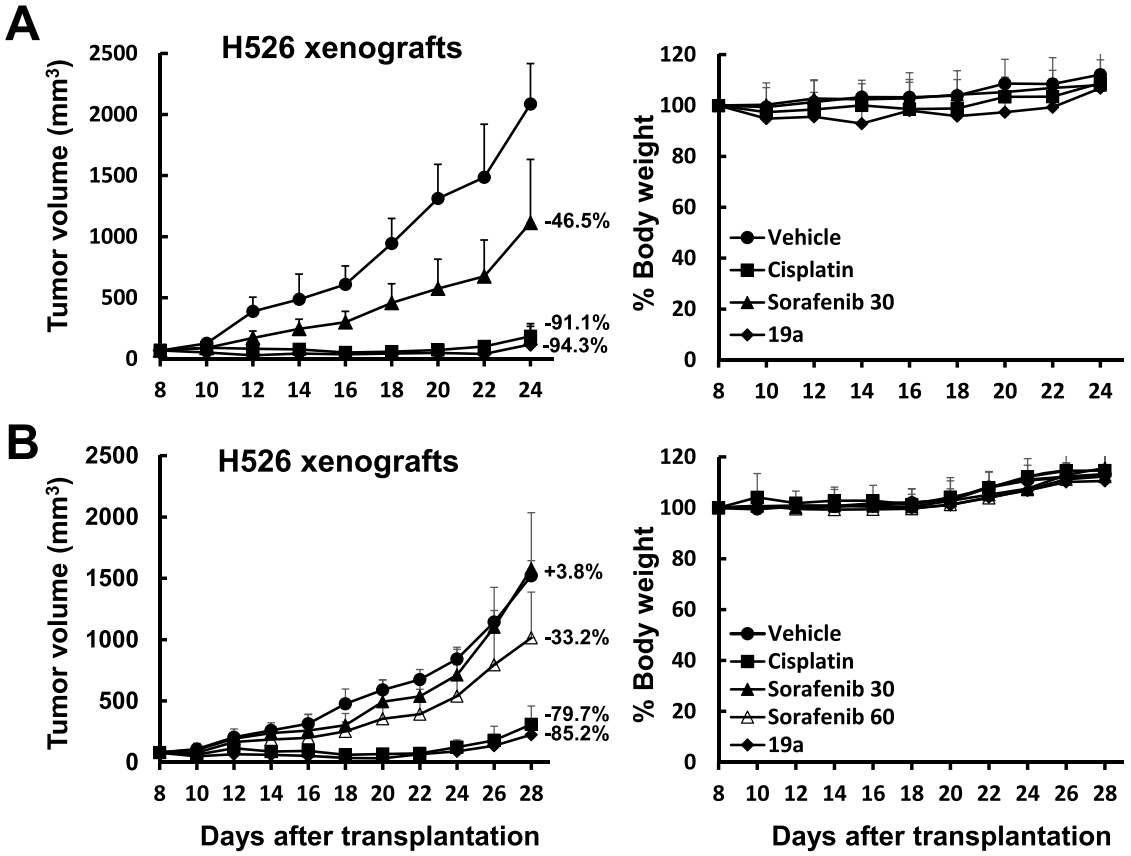

Figure 7. Therapeutic effect of compound **19a** via tail vein injection (A) or per oral administration (B) in nude mice bearing human SCLC H526 xenografts (5 mice in each group). Treatment protocol is described in the Experimental Section. Compound **19a** was administrated via i.v. at the dose of 20 mg/kg (A) or p.o. at 60 mg/kg (B), respectively. The dose of cisplatin was 4 mg/kg, and sorafenib 30 or 60 mg/kg. The numbers indicated the tumor volume changes on day 24 (A) or day 28 (B), respectively.

compared with that of cisplatin (4 mg/kg, Q4D × 3, i.v. injection) and sorafenib (30 mg/kg, 2 cycles of QD × 5 + R, p.o. administration). The results revealed that compound **19a** was more efficacious than cisplatin, as shown in Figure 7A. There was no obvious body weight change in mice treated with compound **19a**.

Oral administration is the most commonly used route of administration because of its safety, simplicity, and convenience.[50] We therefore investigated the therapeutic efficacy of **19a** by p.o. administration using SCLC H526 xenografts. The antitumor potency was determined by treating mice with compound **19a** in a mixture of Tween 80/PEG 400/Kolliphor HS40/ethanol/5% dextrose (2.5:2.5:10:15:70, v/v/v/v/v). Mice bearing H526 xenografts were p.o. administered compound **19a** at 60 mg/kg or sorafenib at 30 or 60 mg/kg for 2 cycles of 5 consecutive days with 1 day of rest (QD × 5 + R) × 2. Cisplatin (4 mg/kg, Q4D × 3, i.v. injection) was also included for comparison. The results shown in Figure 7B revealed that compound **19a** also effectively suppressed the growth of H526 xenografts when administered p.o. Consistently, compound **19a** was more potent than cisplatin on day 32. All compounds examined did not change the body weight of mice during the treatment, indicating that compound **19a** did not induce apparent systemic toxicity under the treatment conditions.

We further examined the efficacy of compound **19a** against renal cell adenocarcinoma 786-O cells and squamous cell carcinoma (SCC) lung cancer H520 cells in mice bearing 786-O and H520 xenografts, respectively. Mice bearing tumor xenografts were orally treated with compound **19a** as described above. Our results revealed that compound **19a** was the most potent agent suppressing the growth of 786-O (Figure 8A) and H520 xenografts (Figure 8B). Similarly, the body weight loss in mice treated with compound **19a** or cisplatin was recovered after the discontinuation of drug treatment. Taken together, our results confirmed that compound **19a** can be developed into an orally available anticancer drug with a broad spectrum.

CONCLUSIONS

We have recently synthesized a series of 1,2-bis-(hydroxymethyl)[2,1-*a*]phthalazine hybrids and demonstrated that compound **4a** exhibited DNA ICL activity and antiangiogenic activity by inhibiting VEGFR-2.[13] Due to its poor solubility, we encapsulated compound **4a** in liposomes and demonstrated its anticancer activity. In this study, we adopted a benzology approach to optimize the efficacy and bioavailability of phthalazine and bis(hydroxymethyl)pyrrole hybrids. We demonstrated that the new hybrid molecules, benzologues of compound **4**, retained multimodal action, including the induction of DNA ICL and suppression of angiogenesis via decreased VEGFR-2 phosphorylation. Although the new hybrids are structurally similar to compound **2** (Figure 1), which possessed the inhibitory activity to topoisomerase I and II,[11] compounds **19a** and **19b** displayed limited inhibition of topoisomerase I and II at the doses of 100 and 50 μM, respectively (Figure S4). These new hybrids were

https://doi.org/10.1021/acs.jmedchem.0c01733
J. Med. Chem. 2021, 64, 12469−12486

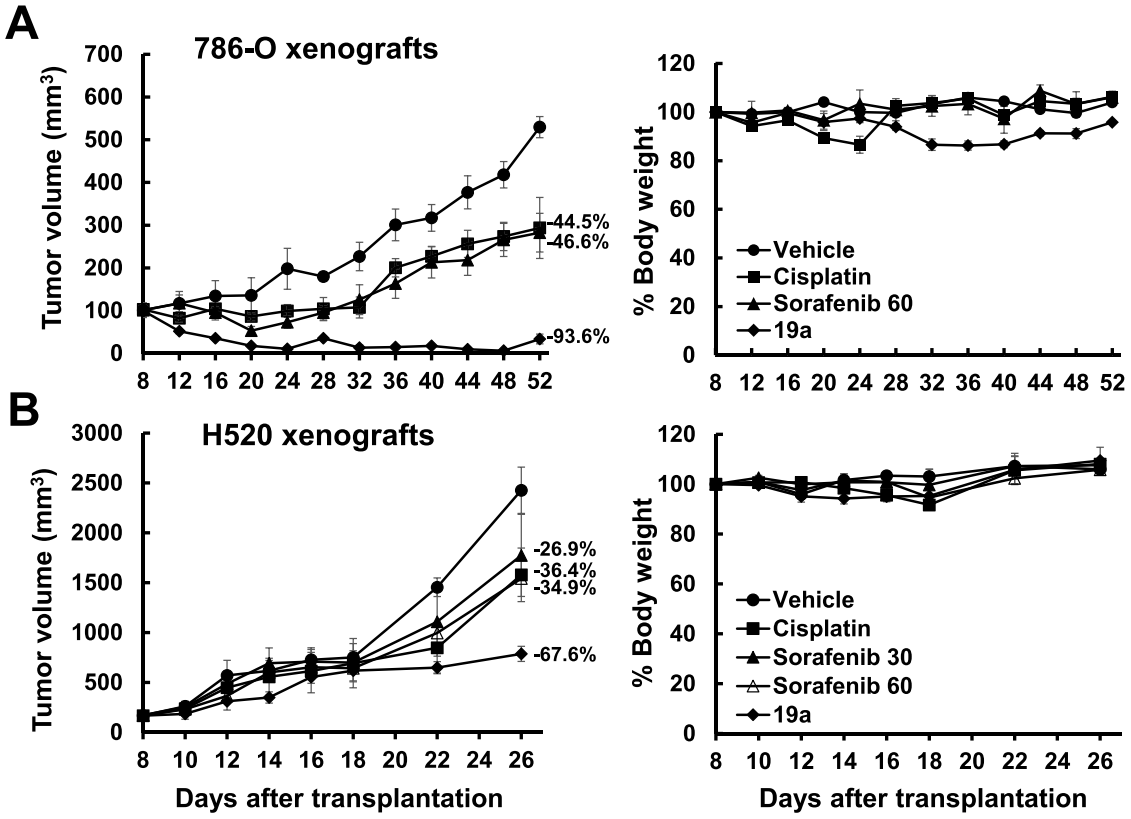

Figure 8. Therapeutic effect of compound **19a** in nude mice bearing human renal cell adenocarcinoma 786-O (A) or lung squamous cell carcinoma H520 (B) xenografts via oral administration (5 mice in each group). Treatment protocol is described in the Experimental Section. Compound **19a** at the dose of 60 mg/kg and sorafenib at 30 or 60 mg/kg was p.o. administrated, while cisplatin at 4 mg/kg was given via tail vein injection. The numbers indicated the tumor volume suppression on day 52 for 786-O (A) or day 26 for H520 (B) xenografts, respectively.

more cytotoxic than their corresponding parent counterparts against a panel of tumor cell lines *in vitro*. They displayed significant cytotoxicity against P-glycoprotein overexpressed human lymphoblastic leukemia (CCRF/CEM) and KB/Vin cells. These compounds also showed strong inhibitory effects against the cell growth of various NSCLC, SCLC, and solid cancer cell lines *in vitro*. Additionally, the solubility of the new hybrids is improved using a new formulation. The new benzophthalazine derivatives are clearly superior to our previously designed phthalazine derivatives.

The SAR studies revealed that compound **19e** with 1,4′-bipiperidine at the C6 position was the most cytotoxic to cell lines tested in culture. However, due to its poor solubility, a new formulation for compound **19e** was required for its further evaluation, which is exactly similar to the results for our previously studied compound **4a**.[13] Fortunately, compound **19a** with dimethylamine at C6 was successfully formulated in vehicles that are available for i.v. and p.o. administration. Our results showed that compound **19a** was more potent than cisplatin in triggering apoptotic death. Among these new hybrids, we also noted that the *in vitro* cytotoxicity of compound **19b** with pyrrolidine at C6 was very similar to that of compound **19a**. The anticancer activity of compound **19b** warrants further investigation.

Combination therapy is a current trend in cancer therapy because of the involvement of multiple molecular pathways in cancer malignancy. The combination of platinum-based drugs, such as cisplatin or carboplatin, with VEGF inhibitors is often used for the treatment of heterogeneous NSCLC and SCLC.[51−54] Although numerous reports have shown promising outcomes in cancer patients receiving antiangiogenic therapy and chemotherapy in combination, several clinical trials showed no improvement.[55−59] The development of advancing chemotherapy regimens through rational drug combinations and discovery of new potent chemotherapeutics remains critical. To improve the efficacy of combination therapy, nanoformulations for combinations of antiangiogenic and chemotherapeutic agents are under development.[60,61] Our results showed that compound **19a** is a broad-spectrum anticancer agent, suggesting that the conjugation of antiangiogenic and DNA ICL moieties may be a novel approach to promote cancer treatment. We propose that the advantage of a compound with two conjugated pharmacophores may be that it can exert both activities at the same location.

The anticancer efficacy of compound **19a** administered via i.v. or p.o. was evaluated in mice bearing various cancer xenografts. Compound **19a** was able to suppress the growth of SCLC cells, squamous lung cancer cells, and renal carcinoma cells in mice, indicating its wide-spectrum anticancer activity. We did not observe a significant body weight change in mice treated with compound **19a**, implicating the low systemic toxicity of compound **19a** to mice. Since compound **19a** could be given via oral administration, it may have certain advantages, such as safety, good patient compliance, ease of ingestion, pain avoidance, and versatility to accommodate various types of drugs.[50] The development of a new formulation for compound **19a** may further advance its clinical application.

In conclusion, we found that the benzology approach is a way to improve phthalazine derivatives. Compound **19a** with

https://doi.org/10.1021/acs.jmedchem.0c01733
J. Med. Chem. 2021, 64, 12469−12486

its antiangiogenic and DNA ICL activities is probably a broad-spectrum anticancer agent. Compound **19a** can be formulated in vehicles available for i.v. and p.o. administration and is a potential candidate for anticancer drug development.

EXPERIMENTAL SECTION

General Chemistry Methods. All commercial chemicals and solvents were of reagent grade and were used without further purification unless otherwise specified. Melting points were determined in open capillaries on a Fargo MP-2D melting point apparatus and are uncorrected. Thin-layer chromatography was performed on silica gel G60 F254 (Merck, Merck KGaA, Darmstadt, Germany) using short-wavelength ultraviolet (UV) light for visualization. ^{1}H NMR spectra and ^{13}C NMR spectra were recorded on Bruker AVANCE Top-Spin spectrometers (400 and 500 MHz) in the solvents indicated. The proton chemical shifts are reported in parts per million (δ ppm) relative to $(CH_3)_4Si$ (TMS), and coupling constants (J) are reported in Hertz (Hz). NMR peak splittings are given by the following abbreviations: s, singlet; d, doublet; dd, double doublet; t, triplet; m, multiplet; and br, broad. HRMS spectra were recorded on a Waters HDMS G1 instrument with ESI$^+$, centroid mode, and the samples were dissolved in MeOH. The reaction at room temperature (rt) is 25 ± 2 °C.

*2,3-Dihydrobenzo[g]phthalazine-1,4-dione (**13**).* Hydrazine hydrate (80% solution, 63 mL) was added to a stirred suspension of naphthalene-2,3-dicarboxylic acid anhydride (**12**) (39.7 g, 200.0 mmol) in glacial acetic acid (600 mL). The mixture was heated at reflux for 6 h with stirring. After cooling, the solid product was collected by filtration, washed with water, and dried to give **13**. Yield: 40.2 g (94%); mp 344−346 °C. ^{1}H NMR (DMSO-d_6): δ 7.75−7.77 (2H, m, ArH), 8.29−8.31 (2H, m, ArH), 8.75 (2H, s, ArH), 11.51 (2H, br s, 2 × NH). ^{13}C NMR (DMSO-d_6): δ 123.8, 126.1, 128.5, 129.1, 134.0. HRMS [ESI$^+$]: calcd for $C_{12}H_8N_2O_2$, 213.0664 [M + H]$^+$, found 213.0681.

*1,4-Dichlorobenzo[g]phthalazine (**14**).* A suspension of **13** (40.0 g, 188.0 mmol) in phosphorus oxychloride (400 mL) containing pyridine (24.0 mL) was heated at 100 °C for 5 h. The reaction mixture was allowed to cool to 40 °C and then concentrated under reduced pressure to dryness. The solid residue was triturated with ether, filtered, and washed with ether. The solid obtained was stirred with ice water for 30 min, and the desired product was collected by filtration, washed with water, and dried to give crude **14**, which was unstable and was used directly for the next reaction. Yield 40.8 g (85%); mp 217−219 °C. ^{1}H NMR (DMSO-d_6): δ 7.91−7.93 (2H, m, ArH), 8.49−8.51 (2H, m, ArH), 9.08 (2H, s, ArH). ^{13}C NMR (DMSO-d_6) δ 124.3, 124.5, 126.2, 126.8, 128.0, 130.0, 137.4, 155.4. HRMS [ESI$^+$]: calcd for $C_{12}H_6Cl_2N_2$, 248.9986 [M + H]$^+$, found 249.0000.

*4-Chloro-N,N-dimethylbenzo[g]phthalazin-1-amine (**15a**).* Dimethylamine (30 mL, 60.0 mmol) was added slowly to a stirred suspension of **14** (10 g, 40.0 mmol) and anhydrous potassium carbonate (55 g, 400.0 mmol) in anhydrous acetonitrile (400 mL) at rt. The reaction mixture was stirred for 72 h at rt and then filtered to remove inorganic salts. The filtrate was evaporated under reduced pressure, and the residue was recrystallized from ether to give **15a**. Yield 9.3 g (90%); mp 90−92 °C; ^{1}H NMR (DMSO-d_6) δ 3.24 (6H, s, $N(CH_3)_2$), 7.79−7.82 (2H, m, ArH), 8.37−8.39 (2H, m, ArH), 8.84 (1H, s, ArH), 8.93 (1H, s, ArH). ^{13}C NMR (DMSO-d_6) δ 42.5, 118.8, 123.1, 125.0, 126.6, 128.6, 128.8, 129.2, 133.9, 134.0, 147.8, 159.7. HRMS [ESI$^+$]: calcd for $C_{14}H_{12}ClN_3$, 258.0798 [M + H]$^+$, found 258.0791.

The following compounds were prepared by the same synthetic procedure as compound **15a**.

*1-Chloro-4-(pyrrolidin-1-yl)benzo[g]phthalazine (**15b**).* Compound **15b** was prepared from **14** (7.0 g, 28.0 mmol) and pyrrolidine (3.5 mL, 42.0 mmol). Yield 6.8 g (85%); mp 112−114 °C. ^{1}H NMR (DMSO-d_6) δ 2.02−2.03 (4H, m, 2 × CH_2), 3.94−3.96 (4H, m, 2 × CH_2), 7.76−7.79 (2H, m, ArH), 8.33−8.38 (2H, m, ArH), 8.75 (1H, s, ArH), 9.06 (1H, s, ArH). ^{13}C NMR (DMSO-d_6) δ 25.4, 51.1, 118.7, 123.1, 123.9, 126.7, 128.1, 128.6, 128.9, 129.4, 133.7, 144.6, 155.5. HRMS [ESI$^+$]: calcd for $C_{16}H_{14}ClN_3$, 284.0955 [M + H]$^+$, found 284.0948.

*1-Chloro-4-(piperidin-1-yl)benzo[g]phthalazine (**15c**).* Compound **15c** was prepared from **14** (5.0 g, 20.0 mmol) and piperidine (4 mL, 40.0 mmol). Yield 3.8 g (64%); mp 128−130 °C. ^{1}H NMR (DMSO-d_6) δ 1.71−1.74 (2H, m, CH_2), 1.83−1.86 (4H, m, 2 × CH_2), 3.47−3.49 (4H, m, 2 × CH_2), 7.79−7.82 (2H, m, ArH), 8.36−8.39 (2H, m, ArH), 8.72 (1H, s, ArH), 8.84 (1H, s, ArH). ^{13}C NMR (DMSO-d_6) δ 24.1, 25.4, 52.1, 119.3, 123.1, 125.4, 125.7, 128.7, 128.9, 129.0, 129.2, 134.1, 149.2, 160.4. HRMS [ESI$^+$]: calcd for $C_{17}H_{16}ClN_3$, 298.1129 [M + H]$^+$, found 298.1144.

*4-(4-Chlorobenzo[g]phthalazin-1-yl)morpholine (**15d**).* Compound **15d** was prepared from **14** (5.0 g, 20.0 mmol) and morpholine (3.5 mL, 40.0 mmol). Yield 3.6 g (60%); mp 125−127 °C. ^{1}H NMR (DMSO-d_6) δ 3.52 (4H, t, J = 4.5 Hz, 2 × CH_2), 3.94 (4H, t, J = 4.5 Hz, 2 × CH_2), 7.80−7.83 (2H, m, ArH), 8.38−8.42 (2H, m, ArH), 8.85 (1H, s, ArH), 8.89 (1H, s, ArH). ^{13}C NMR (DMSO-d_6) δ 51.4, 66.0, 118.9, 123.0, 125.6, 125.8, 128.8, 129.0, 129.1, 129.3, 134.2, 134.3, 149.9, 159.8. HRMS [ESI$^+$]: calcd for $C_{16}H_{14}ClN_3O$, 300.0904 [M + H]$^+$, found 300.0897.

*1-([1,4′-Bipiperidin]-1′-yl)-4-chlorobenzo[g]phthalazine (**15e**).* Compound **15e** was prepared from **14** (7.0 g, 28.0 mmol) and 1,4′-bipiperidine (7.09 g, 42.0 mmol). Yield: 8.5 g (80%); mp 140−142 °C. ^{1}H NMR (DMSO-d_6) δ 1.38−1.41 (2H, m, CH_2), 1.49−1.53 (4H, m, 2 × CH_2), 1.88−1.91 (4H, m, 2 × CH_2), 2.51−2.56 (5H, m, CH and 2 × CH_2), 3.02−3.04 (2H, m, CH_2), 4.00−4.03 (2H, m, CH_2), 7.79−7.82 (2H, m, ArH), 8.37−8.43 (2H, m, ArH), 8.77 (1H, s, ArH), 8.87 (1H, s, ArH). ^{13}C NMR (DMSO-d_6) δ 24.5, 26.0, 27.5, 49.7, 50.8, 61.8, 119.2, 123.1, 125.4, 125.9, 128.7, 128.9, 129.3, 134.2, 149.3, 160.1. HRMS [ESI$^+$]: calcd for $C_{22}H_{25}ClN_4$, 381.1846 [M + H]$^+$, found 381.1826.

*N,N-Dimethylbenzo[g]phthalazin-1-amine (**16a**).* To a solution of **15a** (5.15 g, 20.0 mmol) in MeOH (200 mL) was added 10% Pd/C (1.03 g). The reaction mixture was hydrogenated at 35 psi for 4 h at rt and filtered through a Celite pad. The filter cake was washed well with MeOH. The combined filtrate and washings were concentrated under reduced pressure. The residue was dissolved in DCM (200 mL) and washed with saturated aqueous $NaHCO_3$ solution, dried by anhydrous sodium sulfate, and evaporated in vacuo to dryness. The product was purified by chromatography (SiO_2, elution gradient 0−40% ethyl acetate in hexane) to give **16a**. Yield 2.8 g (64%); mp 115−117 °C. ^{1}H NMR (DMSO-d_6) δ 3.23 (6H, s, $N(CH_3)_2$), 7.73−7.76 (2H, m, ArH), 8.23−8.24 (1H, m, ArH), 8.33−8.35 (1H, m, ArH), 8.68 (1H, s, ArH), 8.85 (1H, s, ArH), 9.26 (1H, s, ArH). ^{13}C NMR (DMSO-d_6) δ 42.4, 117.3, 125.0, 125.1, 126.3, 127.7, 128.1, 128.3, 129.4, 133.7, 133.8, 146.8, 159.0. HRMS [ESI$^+$]: calcd for $C_{14}H_{13}N_3$, 224.1188 [M + H]$^+$, found 224.1198.

The following compounds were synthesized by the same synthetic procedure as **16a**.

*1-(Pyrrolidin-1-yl)benzo[g]phthalazine (**16b**).* Compound **16b** was prepared from **15b** (5.1 g, 18.0 mmol) and 10% Pd/C (1.03 g). Yield 3.3 g (73%); mp 150−152 °C. ^{1}H NMR (DMSO-d_6) δ 2.00−2.03 (4H, m, 2 × CH_2), 3.94−3.97 (4H, m, 2 × CH_2), 7.66−7.72 (2H, m, ArH), 8.17−8.18 (1H, m, ArH), 8.30−8.32 (1H, m, ArH), 8.55 (1H, s, ArH), 8.96 (1H, s, ArH), 9.03 (1H, s, ArH). ^{13}C NMR (DMSO-d_6) δ 25.4, 50.8, 117.2, 125.2, 125.4, 127.1, 128.0, 128.1, 129.6, 133.4, 144.0, 154.8. HRMS [ESI$^+$]: calcd for $C_{16}H_{15}N_3$, 250.1344 [M + H]$^+$, found 250.1362.

*1-(Piperidin-1-yl)benzo[g]phthalazine (**16c**).* Compound **16c** was prepared from **4c** (3.6 g, 12.0 mmol) and 10% Pd/C (0.72 g). Yield 2.0 g (63%); mp 172−174 °C. ^{1}H NMR ($CDCl_3$) δ 1.78−1.80 (2H, m, CH_2), 1.90−1.94 (4H, m, 2 × CH_2), 3.57−3.59 (4H, m, 2 × CH_2), 7.65−7.66 (2H, m, ArH), 8.09−8.13 (2H, m, ArH), 8.43 (1H, s, ArH), 8.59 (1H, s, ArH), 9.24 (1H, s, ArH). ^{13}C NMR ($CDCl_3$) δ 24.8, 26.1, 52.4, 119.0, 124.7, 125.6, 126.5, 127.7, 127.9, 128.5, 129.2, 134.3, 134.4, 148.2, 160.6. HRMS [ESI$^+$]: calcd for $C_{17}H_{17}N_3$, 264.1501 [M + H]$^+$, found 264.1507.

*4-(Benzo[g]phthalazin-1-yl)morpholine (**16d**).* Compound **16d** was prepared from **15d** (2.4 g, 8.0 mmol) and 10% Pd/C (0.48 g).

https://doi.org/10.1021/acs.jmedchem.0c01733
J. Med. Chem. 2021, 64, 12469−12486

Yield 1.1 g (52%); mp 180−182 °C. ^{1}H NMR (DMSO-d_6) δ 3.51−3.53 (4H, m, 2 × CH_2), 3.94−3.96 (4H, m, 2 × CH_2), 7.75−7.76 (2H, m, ArH), 8.25−8.26 (1H, m, ArH), 8.38−8.39 (1H, m, ArH),8.75 (1H, s, ArH), 8.81 (1H, s, ArH), 9.39 (1H, s, ArH). ^{13}C NMR (DMSO-d_6) δ 51.3, 66.1, 117.4, 124.3, 124.9, 126.9, 127.9, 128.3, 128.5, 129.4, 133.9, 134.1, 148.4, 159.0. HRMS [ESI$^+$]: calcd for $C_{16}H_{15}N_3O$, 266.1293 [M + H]$^+$, found 266.1304.

*1-([1,4′-bipiperidin]-1′-yl)benzo[g]phthalazine (**16e**).* Compound **16e** was prepared from **15e** (3.82 g, 10.0 mmol) and 10% Pd/C (0.76 g). Yield 1.8 g (52%); mp 165−167 °C. ^{1}H NMR ($CDCl_3$) δ 1.47−1.48 (2H, m, CH_2), 1.62−1.66 (4H, m, 2 × CH_2), 1.91−1.99 (2H, m, CH_2), 2.06−2.08 (2H, m, CH_2), 2.54−2.56 (1H, m, CH), 2.58−2.63 (4H, m, 2 × CH_2), 3.08−3.13 (2H, m, CH_2), 4.12−4.14 (2H, m, CH_2), 7.64−7.66 (2H, m, ArH), 8.07−8.12 (2H, m, ArH), 8.42 (1H, s, ArH), 8.55 (1H, s, ArH), 9.23 (1H, s, ArH). ^{13}C NMR ($CDCl_3$) δ 24.7, 26.3, 28.3, 50.4, 51.1, 62.7, 118.8, 124.5, 125.4, 126.5, 127.8, 127.9, 128.5, 129.1, 134.3, 134.4, 148.3, 160.1. HRMS [ESI$^+$]: calcd for $C_{22}H_{26}N_4$, 347.2236 [M + H]$^+$, found 347.2254.

*2-Acetyl-4-(dimethylamino)-1,2-dihydrobenzo[g]phthalazine-1-carbonitrile (**17a**).* To a solution of **16a** (2.2 g, 10.0 mmol) in DCM (30 mL) containing a catalytic amount of $AlCl_3$, Me_3SiCN (2.5 mL, 20.0 mmol) was added dropwise. Acetyl chloride (1.1 mL, 15.0 mmol) was added dropwise to the above mixture and then stirred for 4 h at rt. The reaction mixture was poured into ice water, and the organic layer was washed successively with water, 5% NaOH solution, and water. The solution was dried over sodium sulfate and concentrated under vacuum to give **17a**. Yield 2.7 g (92%); mp 125−127 °C. ^{1}H NMR (DMSO-d_6) δ 2.27 (3H, s, $COCH_3$), 2.98 (6H, s, $N(CH_3)_2$), 7.21 (1H, s, CH), 7.66−7.72 (2H, m, ArH), 8.01 (1H, m, ArH), 8.18 (1H, m, ArH), 8.33 (2H, s, ArH). ^{13}C NMR (DMSO-d_6) δ 20.6, 40.9, 116.4, 118.2, 125.8, 126.3, 127.3, 127.7, 127.8, 128.8, 129.4, 132.8, 133.7, 155.7, 170.9. HRMS [ESI$^+$]: calcd for $C_{17}H_{16}N_4O$, 293.1402 [M + H]$^+$, found 293.1407.

The following compounds were synthesized by the same synthetic procedure as **17a**.

*2-Acetyl-4-(pyrrolidin-1-yl)-1,2-dihydrobenzo[g]phthalazine-1-carbonitrile (**17b**).* Compound **17b** was prepared from **16b** (3.25 g, 13.0 mmol), Me_3SiCN (3.26 mL, 26.0 mmol) and acetyl chloride (1.4 mL, 19.6 mmol). Yield 3.2 g (77%); mp 162−164 °C. ^{1}H NMR ($CDCl_3$) δ 1.92−1.99 (2H, m, CH_2), 2.07−2.10 (2H, m, CH_2), 2.31 (3H, s, $COCH_3$), 3.43−3.47 (2H, m, CH_2), 3.83−3.88 (2H, m, CH_2), 6.90 (1H, s, CH), 7.58−7.64 (2H, m, ArH), 7.85 (1H, s, ArH), 7.88−7.90 (1H, m, ArH), 7.92−7.93 (1H, m, ArH), 8.17 (1H, s, ArH). ^{13}C NMR ($CDCl_3$) δ 20.6, 25.4, 41.5, 50.0, 115.8, 120.1, 125.7, 126.3, 126.9, 127.6, 127.8, 128.5, 128.9, 133.1, 133.7, 154.0. 171.0. HRMS [ESI$^+$]: calcd for $C_{19}H_{18}N_4O$, 319.1559 [M + H]$^+$, found 319.1557.

*2-Acetyl-4-(piperidin-1-yl)-1,2-dihydrobenzo[g]phthalazine-1-carbonitrile (**17c**).* Compound **17c** was prepared from **16c** (1.85 g, 7.0 mmol), Me_3SiCN (1.8 mL, 14.0 mmol) and acetyl chloride (0.8 mL, 10.5 mmol). Yield 2.1 g (90%); mp 181−183 °C. ^{1}H NMR (DMSO-d_6) δ 1.66 (4H, m, 2 × CH_2), 1.89−1.91 (2H, m, CH_2), 2.28 (3H, s, $COCH_3$), 3.15−3.19 (2H, m, CH_2), 3.41−3.45 (2H, m, CH_2), 7.22 (1H, s, CH), 7.66−7.72 (2H, m, ArH), 8.00−8.01 (1H, m, ArH), 8.20−8.22 (1H, m, ArH), 8.22 (1H, s, ArH), 8.34 (1H, s, ArH). ^{13}C NMR (DMSO-d_6) δ 20.6, 24.1, 24.8, 40.4, 50.2, 116.3, 118.2, 125.8, 126.3, 126.7, 127.7, 127.8, 128.7, 129.5, 132.8, 133.7, 155.4, 171.0. HRMS [ESI$^+$]: calcd for $C_{20}H_{20}N_4O$, 333.1715 [M + H]$^+$, found 333.1720.

*2-Acetyl-4-morpholino-1,2-dihydrobenzo[g]phthalazine-1-carbonitrile (**17d**).* Compound **17d** was prepared from **16d** (1.07 g, 4.0 mmol), Me_3SiCN (1.0 mL, 8.0 mmol) and acetyl chloride (0.43 mL, 6.0 mmol). Yield 1.24 g (92%); mp 190−192 °C. ^{1}H NMR (DMSO-d_6) δ 2.28 (3H, s, $COCH_3$), 3.09−3.34 (2H, m, CH_2), 3.46−3.51 (2H, m, CH_2), 3.75−3.79 (2H, m, CH_2), 3.96−4.01 (2H, m, CH_2), 7.23 (1H, s, CH), 7.66−7.73 (2H, m, ArH), 8.00−8.02 (1H, m, ArH), 8.21−8.22 (1H, m, ArH), 8.29 (1H, s, ArH), 8.34 (1H, s, ArH). ^{13}C NMR (DMSO-d_6) δ 20.6, 49.7, 65.6, 116.3, 117.5 125.6, 126.5, 126.9, 127.7, 127.8, 128.8, 129.5, 132.8, 133.8, 154.6, 171.1. HRMS [ESI$^+$]: calcd for $C_{19}H_{18}N_4O_2$, 335.1508 [M + H]$^+$, found 335.1516.

*4-([1,4′-Bipiperidin]-1′-yl)-2-acetyl-1,2-dihydrobenzo[g]-phthalazine-1-carbonitrile (**17e**).* Compound **17e** was prepared from **16e** (1.75 g, 5.0 mmol), Me_3SiCN (1.26 mL, 10.0 mmol) and acetyl chloride (0.54 mL, 7.5 mmol). Yield 1.8 g (86%); mp 205−207 °C. ^{1}H NMR ($CDCl_3$) δ 1.46−1.47 (2H, m, CH_2), 1.59−1.64 (4H, m, 2 × CH_2), 1.66−1.75 (1H, m, CH_2), 1.94−2.02 (3H, m, CH_2), 2.32 (3H, s, $COCH_3$), 2.45−2.52 (1H, m, CH), 2.58 (4H, br s, 2 × CH_2), 2.69−2.75 (1H, m, CH_2), 3.01−3.06 (1H, m, CH_2), 3.75−3.78 (1H, m, CH_2), 3.96−3.98 (1H, m, CH_2), 6.83 (1H, s, CH), 7.57−7.63 (2H, m, ArH), 7.84 (1H, s, ArH), 7.87−7.89 (1H, m, ArH), 7.92−7.93 (1H, m, ArH), 8.03 (1H, s, ArH). ^{13}C NMR (DMSO-d_6) δ 20.8, 24.7, 26.3, 27.6, 27.8, 41.0, 47.9, 50.3, 51.0, 62.5, 115.5, 118.9, 125.8, 125.9, 126.9, 127.7, 127.9, 128.6, 129.1, 133.3, 134.2, 155.8, 171.5. HRMS [ESI$^+$]: calcd for $C_{25}H_{29}N_5O$, 416.2450 [M + H]$^+$, found 416.2471. Since compound **17e** has a chiral center, the resolution of its ^{1}H NMR spectrum remains to be solved.

*Dimethyl 6-(dimethylamino)-3-methylbenzo[g]pyrrolo[2,1-a]-phthalazine-1,2-dicarboxylate (**18a**).* To a solution of **17a** (2.9 g, 10.0 mmol) in warm acetic acid (50 mL), HBF_4 (2.2 mL, 12.0 mmol) was added dropwise. The mixture was stirred at 50−60 °C for 30 min. After cooling to rt, the yellow solid salt was collected by filtration, and the filter cake was washed with dry ether. The solid salt was dissolved in DMF (20 mL), and DMAD (3.1 mL, 25.0 mmol) was slowly added to this solution. The reaction mixture was heated at 90−100 °C for 16 h. The solvent was removed by evaporation in vacuo. The residue was crystallized from MeOH to give **18a**. Yield 1.7 g (43%); mp 180−182 °C. ^{1}H NMR (DMSO-d_6) δ 2.65 (3H, s, CH_3), 3.07 (6H, s, $N(CH_3)_2$), 3.80 (3H, s, $COOCH_3$), 3.96 (3H, s, $COOCH_3$), 7.62−7.64 (1H, m, ArH), 7.69−7.72 (1H, m, ArH), 8.05−8.07 (1H, m, ArH), 8.22−8.24 (1H, m, ArH), 8.65 (1H, s, ArH), 8.72 (1H, s, ArH). ^{13}C NMR (DMSO-d_6) δ 10.1, 42.6, 51.6, 52.5, 107.9, 111.1, 115.6, 119.9, 121.0, 123.8, 126.9, 127.8, 128.0, 128.9, 129.4, 130.8, 131.2, 134.0, 156.8, 164.4, 166.8. HRMS [ESI$^+$]: calcd for $C_{22}H_{21}N_3O_4$, 392.1610 [M + H]$^+$, found 392.1590.

The following compounds were prepared by the same synthetic procedure as **18a**.

*Dimethyl 3-methyl-6-(pyrrolidin-1-yl)benzo[g]pyrrolo[2,1-a]-phthalazine-1,2-dicarboxylate (**18b**).* Compound **18b** was prepared from **17b** (3.2 g, 10.0 mmol), HBF_4 (2.2 mL, 12.0 mmol) and DMAD (3.1 mL, 25.0 mmol). Yield 2.0 g (48%); mp 190−192 °C. ^{1}H NMR ($CDCl_3$) δ 2.02−2.04 (4H, m, 2 × CH_2), 2.68 (3H, s, CH_3), 3.75−3.78 (4H, m, 2 × CH_2), 3.88 (3H, s, $COOCH_3$), 4.03 (3H, s, $COOCH_3$), 7.49−7.51 (1H, m, ArH), 7.55−7.58 (1H, m, ArH), 7.89−7.93 (2H, m, ArH), 8.52 (1H, s, ArH), 8.77 (1H, s, ArH). ^{13}C NMR ($CDCl_3$) δ 10.4, 25.6, 51.4, 51.5, 52.4, 107.5, 111.1, 117.0, 120.6, 121.8, 124.8, 126.3, 127.1, 128.1, 128.2, 128.8, 131.1, 131.3, 134.3, 153.8, 165.5, 168.1. HRMS [ESI$^+$]: calcd for $C_{24}H_{23}N_3O_4$, 444.1586 [M + Na]$^+$, found 444.1569.

*Dimethyl 3-methyl-6-(piperidin-1-yl)benzo[g]pyrrolo[2,1-a]-phthalazine-1,2-dicarboxylate (**18c**).* Compound **18c** was prepared from **17c** (2.0 g, 6.0 mmol), HBF_4 (1.6 mL, 7.2 mmol) and DMAD (1.85 mL, 15.0 mmol). Yield 1.2 g (46%); mp 200−202 °C. ^{1}H NMR ($CDCl_3$) δ 1.73−1.75 (2H, m, CH_2), 1.86−1.89 (4H, m, 2 × CH_2), 2.72 (3H, s, CH_3), 3.33−3.35 (4H, m, 2 × CH_2), 3.89 (3H, s, $COOCH_3$), 4.04 (3H, s, $COOCH_3$), 7.52−7.58 (2H, m, ArH), 7.95−7.96 (2H, m, ArH), 8.44 (1H, s, ArH), 8.79 (1H, s, ArH). ^{13}C NMR ($CDCl_3$) δ 10.3, 24.6, 25.8, 51.5, 52.4, 52.6, 107.9, 111.6, 116.5, 121.0, 122.2, 124.6, 126.4, 126.7, 128.1, 128.3, 128.9, 131.5, 132.1, 134.7, 157.2, 165.4, 167.9. HRMS [ESI$^+$]: calcd for $C_{25}H_{25}N_3O_4$, 432.1923 [M + H]$^+$, found 432.1904.

*Dimethyl 3-methyl-6-morpholinobenzo[g]pyrrolo[2,1-a]-phthalazine-1,2-dicarboxylate (**18d**).* Compound **18d** was prepared from **17d** (1.17 g, 3.5 mmol), HBF_4 (0.77 mL, 4.2 mmol) and DMAD (1.1 mL, 8.7 mmol). Yield 0.8 g (53%); mp 226−228 °C. ^{1}H NMR ($CDCl_3$) δ 2.72 (3H, s, CH_3), 3.40−3.42 (4H, m, 2 × CH_2), 3.90 (3H, s, $COOCH_3$), 4.01−4.03 (4H, m, 2 × CH_2), 4.04 (3H, s, $COOCH_3$), 7.52−7.55 (1H, m, ArH), 7.58−7.61 (1H, m, ArH), 7.94−7.97 (2H, m, ArH), 8.43 (1H, s, ArH), 8.82 (1H, s, ArH). ^{13}C NMR ($CDCl_3$) δ 10.3, 51.6, 51.7, 52.5, 66.7, 108.2, 112.0, 115.8, 121.0, 122.4, 124.5, 126.4, 126.7, 128.3, 128.4, 128.8, 131.4, 132.2,

https://doi.org/10.1021/acs.jmedchem.0c01733
J. Med. Chem. 2021, 64, 12469−12486

134.8, 156.1, 165.3, 167.7. HRMS [ESI$^+$]: calcd for $C_{24}H_{23}N_3O_5$, 456.1535 [M + Na]$^+$, found 456.1512.

*Dimethyl 6-([1,4′-bipiperidin]-1′-yl)-3-methylbenzo[g]pyrrolo-[2,1-a]phthalazine-1,2-dicarboxylate (**18e**).* Compound **18e** was prepared from **17e** (1.7 g, 4.0 mmol), HBF_4 (0.9 mL, 4.8 mmol) and DMAD (1.23 mL, 10.0 mmol). Yield 0.95 g (45%); mp 260−262 °C. ^{1}H NMR (DMSO-d_6) δ 1.47 (1H, br s, CH_2), 1.74 (3H, br s, CH_2), 1.88 (2H, br s, CH_2), 2.08−2.15 (4H, m, 2 × CH_2), 2.65 (3H, s, CH_3), 3.03−3.07 (4H, m, 2 × CH_2), 3.50 (3H, br s, CH and CH_2), 3.81 (3H, s, $COOCH_3$), 3.93−3.95 (2H, m, CH_2), 3.97 (3H, s, $COOCH_3$), 7.64−7.67 (1H, m, ArH), 7.69−7.72 (1H, m, ArH), 8.06−8.07 (1H, m, ArH), 8.18−8.20 (1H, m, ArH), 8.58 (1H, s, ArH), 8.66 (1H, s, ArH). ^{13}C NMR (DMSO-d_6) δ 10.1, 23.0, 25.5, 49.2, 49.6, 51.6, 52.5, 108.1, 111.4, 115.4, 120.0, 121.3, 123.7, 127.1, 127.3, 128.0, 129.0, 129.3, 131.0, 131.3, 134.2, 155.8, 164.3, 166.7. HRMS [ESI$^+$]: calcd for $C_{30}H_{34}N_4O_4$, 515.2658 [M + H]$^+$, found 515.2685.

*(6-(Dimethylamino)-3-methylbenzo[g]pyrrolo[2,1-a]-phthalazine-1,2-diyl)dimethanol (**19a**).* A solution of **18a** (1.6 g, 4.0 mmol) in DCM (50 mL) was added dropwise to a stirred suspension of LAH (0.39 g, 10.0 mmol) in diethyl ether (20 mL) at 0−5 °C. After completion of the reaction (2 h), the excess LAH was decomposed by the addition of water (2 mL) and NH_4OH (2 mL). The reaction mixture was then filtered through a Celite pad and washed well with DCM. The combined filtrate and washings were concentrated to dryness in vacuo. The residue was crystallized from ethanol to give **19a**. Yield 1.1 g (80%); mp 156−158 °C. ^{1}H NMR (DMSO-d_6) δ 2.46 (3H, s, CH_3), 2.99 (6H, s, $N(CH_3)_2$), 4.56 (2H, d, J = 5.0 Hz, OCH_2), 4.61 (1H, t, J = 5.0 Hz, OH, exchangeable), 4.89−4.90 (3H, m, OCH_2 and OH, exchangeable), 7.51−7.53 (1H, m, ArH), 7.61−7.64 (1H, m, ArH), 7.99−8.01 (1H, m, ArH), 8.13−8.14 (1H, m, ArH), 8.58 (1H, s, ArH), 8.66 (1H, s, ArH). ^{13}C NMR (DMSO-d_6) δ 8.9, 42.8, 53.3, 54.1, 115.6, 115.7, 117.5, 120.3, 120.4, 123.5, 125.5, 126.3, 126.2, 127.4, 128.1, 129.2, 130.0, 134.5, 154.7. HRMS [ESI$^+$]: calcd for $C_{20}H_{21}N_3O_2$, 318.1606 [M + H − H_2O]$^+$, found 318.1620.

The following compounds were prepared by the same synthetic procedure as **19a**.

*(3-Methyl-6-(pyrrolidin-1-yl)benzo[g]pyrrolo[2,1-a]phthalazine-1,2-diyl)dimethanol (**19b**).* Compound **19b** was prepared from **18b** (1.7 g, 4.0 mmol) and LAH (0.39 g, 10.0 mmol). Yield 1.1 g (82%); mp160−162 °C. ^{1}H NMR (DMSO-d_6) δ 1.97−1.99 (4H, m, 2 × CH_2), 2.42 (3H, s, CH_3), 3.67−3.70 (4H, m, 2 × CH_2), 4.51−4.55 (3H, m, OCH_2 and OH, exchangeable), 4.82 (1H, t, J = 5.0 Hz, OH, exchangeable), 4.89 (2H, d, J = 5.0 Hz, OCH_2), 7.48−7.51 (1H, m, ArH), 7.59−7.62 (1H, m, ArH), 7.97−7.98 (1H, m, ArH), 8.13−8.14 (1H, m, ArH), 8.63 (1H, s, ArH), 8.66 (1H, s, ArH). ^{13}C NMR (DMSO-d_6) δ 8.9, 24.9, 50.9, 53.3, 54.2, 115.1, 116.4, 117.2, 119.8, 119.9, 122.9, 125.2, 126.3, 126.7, 127.2, 128.0, 129.2, 129.8, 134.3, 152.2. HRMS [ESI$^+$]: calcd for $C_{22}H_{23}N_3O_2$, 344.1763 [M + H − H_2O]$^+$, found 344.1754.

*(3-Methyl-6-(piperidin-1-yl)benzo[g]pyrrolo[2,1-a]phthalazine-1,2-diyl)dimethanol (**19c**).* Compound **19c** was prepared from **18c** (1.1 g, 2.5 mmol) and LAH (0.24 g, 6.3 mmol). Yield 0.83 g (86%); mp 173−175 °C. ^{1}H NMR (DMSO-d_6) δ 1.68−1.69 (2H, m, CH_2), 1.84−1.85 (4H, m, 2 × CH_2), 2.45 (3H, s, CH_3), 3.24−3.26 (4H, m, 2 × CH_2), 4.56−4.60 (3H, m, OCH_2 and OH, exchangeable), 4.87 (1H, t, J = 5.0 Hz, OH, exchangeable), 4.91 (2H, d, J = 5.0 Hz, OCH_2), 7.50−7.53 (1H, m, ArH), 7.60−7.63 (1H, m, ArH), 7.99−8.01 (1H, m, ArH), 8.12−8.14 (1H, m, ArH), 8.47 (1H, s, ArH), 8.66 (1H, s, ArH). ^{13}C NMR (DMSO-d_6) δ 8.8, 24.2, 25.1, 25.4, 52.3, 53.3, 54.1, 67.0, 115.6, 115.7, 117.5, 120.4, 123.5, 125.4, 125.9, 126.2, 127.4, 128.0, 129.2, 130.0, 134.6, 154.7. HRMS [ESI$^+$]: calcd for $C_{23}H_{25}N_3O_2$, 376.2025 [M + H]$^+$, found 376.1996.

*(3-Methyl-6-morpholinobenzo[g]pyrrolo[2,1-a]phthalazine-1,2-diyl)dimethanol (**19d**).* Compound **19d** was prepared from **18d** (0.65 g, 1.5 mmol) and LAH (0.14 g, 3.75 mmol). Yield: 0.46 g (82%); mp 190−192 °C. ^{1}H NMR (DMSO-d_6) δ 2.46 (2H, s, CH_3), 3.28−3.30 (4H, m, 2 × CH_2), 3.92−3.94 (4H, m, 2 × CH_2), 4.56 (2H, d, J = 5.5 Hz, OCH_2), 4.61 (1H, t, J = 5.5 Hz, OH, exchangeable), 4.89 (1H, t, J = 5.0 Hz, OH, exchangeable), 4.92 (2H, d, J = 5.0 Hz, OCH_2), 7.50−7.53 (1H, m, ArH), 7.61−7.64 (1H, m, ArH), 8.00−8.01 (1H, m, ArH), 8.15−8.16 (1H, m, ArH), 8.55 (1H, s, ArH), 8.67 (1H, s, ArH). ^{13}C NMR (DMSO-d_6) δ 8.8, 51.6, 53.3, 54.1, 66.0, 115.1, 115.8, 117.5, 120.5, 123.6, 125.5, 126.0, 126.1, 127.4, 128.1, 129.3, 130.0, 134.6, 153.7. HRMS [ESI$^+$]: calcd for $C_{22}H_{23}N_3O_3$, 360.1712 [M + H − H_2O]$^+$, found 360.1711.

*(6-([1,4′-Bipiperidin]-1′-yl)-3-methylbenzo[g]pyrrolo[2,1-a]-phthalazine-1,2-diyl)dimethanol (**19e**).* Compound **19e** was prepared from **18e** (0.67 g, 1.3 mmol) and LAH (0.12 g, 3.25 mmol). Yield 0.45 g (76%); mp 181−183 °C. ^{1}H NMR (DMSO-d_6) δ 1.42 (2H, br s, CH_2), 1.53 (4H, br s, 2 × CH_2), 1.89 (4H, br s, 2 × CH_2), 2.44 (3H, s, CH_3), 2.55 (5H, m, CH and 2 × CH_2), 2.85−2.89 (2H, m, CH_2), 3.71−3.73 (2H, m, CH_2), 4.55−4.60 (3H, m, OCH_2 and OH, exchangeable), 4.89−4.90 (3H, m, OCH_2 and OH, exchangeable), 7.51−7.53 (1H, m, ArH), 7.61−7.63 (1H, m, ArH), 7.99−8.01 (1H, m, ArH), 8.15−8.17 (1H, m, ArH), 8.48 (1H, s, ArH), 8.65 (1H, s, ArH). ^{13}C NMR (DMSO-d_6) δ 13.5, 16.6, 24.5, 25.0, 26.0, 27.3, 49.6, 50.9, 53.0, 53.9, 61.8, 66.9, 113.6, 115.6, 117.5, 120.3, 123.0, 124.7, 125.5, 128.2, 129.7, 131.6, 153.9. HRMS [ESI$^+$]: calcd for $C_{28}H_{34}N_4O_2$, 459.2760 [M + H]$^+$, found 459.2728.

*(6-(Dimethylamino)-3-methylbenzo[g]pyrrolo[2,1-a]-phthalazine-1,2-diyl)-bis(methylene) bis(ethylcarbamate) (**20a**).* Ethyl isocyanate (0.2 mL, 2.4 mmol) was added to a solution of **19a** (0.2 g, 0.6 mmol) and TEA (0.55 mL, 4.0 mmol) in dry DMF. The reaction mixture was stirred for 24−48 h at rt under argon. After completion of the reaction, the reaction mixture was concentrated to dryness in vacuo. The residue was triturated with ether, and the desired product **20a** was collected by filtration. Yield 0.15 g (53%); mp 132−134 °C. ^{1}H NMR (DMSO-d_6) δ 0.99 (6H, t, J = 7.0 Hz, 2 × CH_3), 2.48 (3H, s, CH_3), 2.98−3.02 (10H, m, 2 × CH_2 and $N(CH_3)_2$), 5.18 (2H, s, OCH_2), 5.49 (2H, s, OCH_2), 7.04−7.06 (1H, br s, NH, exchangeable), 7.09−7.11 (1H, br s, NH, exchangeable), 7.54−7.57 (1H, m, ArH), 7.64−7.67 (1H, m, ArH), 7.96−7.98 (1H, m, ArH), 8.16−8.18 (1H, m, ArH), 8.50 (1H, s, ArH), 8.63 (1H, s, ArH). ^{13}C NMR (DMSO-d_6). δ 8.9, 15.1, 15.2, 35.0, 35.1, 42.7, 56.1, 56.9, 110.6, 115.5, 116.2, 118.5, 120.2, 125.4, 125.5, 125.9, 127.0, 127.5, 128.3, 129.2, 130.3, 134.5, 155.2, 156.1, 156.3. HRMS [ESI$^+$]: calcd for $C_{26}H_{31}N_5O_4$, 302.1657 [M + H − 2($OCONHC_2H_5$)]$^+$, found 302.1667.

The following compounds were prepared by the same procedure as **20a**.

*(3-Methyl-6-(pyrrolidin-1-yl)benzo[g]pyrrolo[2,1-a]phthalazine-1,2-diyl)-bis(methylene) bis(ethylcarbamate) (**20b**).* Compound **20b** was prepared from **19b** (0.36 g, 1.0 mmol), ethyl isocyanate (0.32 mL, 4.0 mmol), and TEA (0.55 mL, 4.0 mmol). Yield 0.28 g (56%); mp 142−144 °C. ^{1}H NMR (DMSO-d_6) δ 0.96 (3H, t, J = 7.0 Hz, CH_3), 1.00 (3H, t, J = 7.0 Hz, CH_3), 1.96−1.99 (4H, m, 2 × CH_2), 2.44 (3H, s, CH_3), 2.96−3.06 (4H, m, 2 × CH_2), 3.69−3.72 (4H, m, 2 × CH_2), 5.16 (2H, s, OCH_2), 5.47 (2H, s, OCH_2), 7.02 (1H, t, J = 5.5 Hz, NH, exchangeable), 7.07 (1H, t, J = 5.5 Hz, NH, exchangeable), 7.52−7.55 (1H, m, ArH), 7.63−7.66 (1H, m, ArH), 7.93−7.94 (1H, m, ArH), 8.16−8.17 (1H, m, ArH), 8.46 (1H, s, ArH), 8.72 (1H, s, ArH). ^{13}C NMR (DMSO-d_6) δ 8.9, 15.0, 15.1, 25.1, 35.0, 35.1, 50.9, 56.2, 57.0, 109.9, 115.7, 116.3, 118.2, 119.8, 124.8, 125.7, 127.1, 127.3, 128.2, 129.3, 130.1, 134.2, 152.6, 156.1, 156.3. HRMS [ESI$^+$]: calcd for $C_{28}H_{33}N_5O_4$, 328.1814 [M + H − 2($OCONHC_2H_5$)]$^+$, found 328.1816.

*(3-Methyl-6-(piperidin-1-yl)benzo[g]pyrrolo[2,1-a]phthalazine-1,2-diyl)-bis(methylene) bis(ethylcarbamate) (**20c**).* Compound **20c** was prepared from **19c** (0.3 g, 0.8 mmol), ethyl isocyanate (0.25 mL, 3.2 mmol), and TEA (0.45 mL, 3.2 mmol). Yield 0.28 g (68%); mp160−162 °C. ^{1}H NMR (DMSO-d_6) δ 0.96−1.01 (6H, m, 2 × CH_3), 1.58 (2H, br s, CH_2), 1.84−1.85 (4H, m, 2 × CH_2), 2.47 (3H, s, CH_3), 2.95−3.05 (4H, m, 2 × CH_2), 3.24 (4H, br s, 2 × CH_2), 5.17 (2H, s, OCH_2), 5.49 (2H, s, OCH_2), 7.03 (1H, t, J = 5.5 Hz, NH, exchangeable), 7.07 (1H, t, J = 5.5 Hz, NH, exchangeable), 7.54−7.57 (1H, m, ArH), 7.64−7.67 (1H, m, ArH), 7.96−7.98 (1H, m, ArH), 8.16−8.18 (1H, m, ArH), 8.51 (1H, s, ArH), 8.52 (1H, s, ArH). ^{13}C NMR (DMSO-d_6) δ 8.8, 15.0, 15.1, 24.1, 25.4, 35.0, 35.1, 52.3, 56.1,

https://doi.org/10.1021/acs.jmedchem.0c01733
J. Med. Chem. 2021, 64, 12469−12486

56.9, 110.6, 115.6, 116.3, 118.5, 120.3, 125.5, 125.9, 126.3, 127.5, 128.2, 129.2, 130.2, 134.5, 155.2, 156.0, 156.2. HRMS [ESI$^+$]: calcd for $C_{29}H_{35}N_5O_4$, 342.1970 [M + H − 2(OCONHC$_2$H$_5$)]$^+$, found 342.1959.

*(3-Methyl-6-morpholinobenzo[g]pyrrolo[2,1-a]phthalazine-1,2-diyl)bis-(methylene) bis(ethylcarbamate) (**20d**).* Compound **20d** was prepared from **19d** (0.3 g, 0.8 mmol), ethyl isocyanate (0.25 mL, 3.2 mmol), and TEA (0.45 mL, 3.2 mmol). Yield 0.3 g (73%); mp 178−180 °C. ^{1}H NMR (DMSO-d_6) δ 0.98 (3H, t, J = 7.0 Hz, CH$_3$), 1.00 (3H, t, J = 7.0 Hz, CH$_3$), 2.48 (3H, s, CH$_3$), 2.94−3.05 (4H, m, 2 × CH$_2$), 3.31−3.36 (4H, m, 2 × CH$_2$), 3.93−3.95 (4H, m, 2 × CH$_2$), 5.18 (2H, s, OCH$_2$), 5.50 (2H, s, OCH$_2$), 7.03 (1H, t, J = 5.5 Hz, NH, exchangeable), 7.07 (1H, t, J = 5.5 Hz, NH, exchangeable), 7.55−7.58 (1H, m, ArH), 7.65−7.67 (1H, m, ArH), 7.97−7.98 (1H, m, ArH), 8.18−8.20 (1H, m, ArH), 8.53 (1H, s, ArH), 8.61 (1H, s, ArH). ^{13}C NMR (DMSO-d_6) δ 9.3, 15.5, 15.6, 35.5, 52.0, 56.5, 66.4, 111.3, 115.5, 116.9, 119.1, 120.9, 125.9, 126.4, 126.9, 128.1, 128.8, 129.8, 130.8, 135.0, 154.8, 154.9, 156.5, 156.7. HRMS [ESI$^+$]: calcd for $C_{28}H_{33}N_5O_5$, 344.1763 [M + H − 2(OCONHC$_2$H$_5$)]$^+$, found 344.1718.

*(6-([1,4′-Bipiperidin]-1′-yl)-3-methylbenzo[g]pyrrolo[2,1-a]-phthalazine-1,2-diyl)bis(methylene) bis(ethylcarbamate) (**20e**).* Compound **20e** was prepared from **19e** (0.23 g, 0.5 mmol), ethyl isocyanate (0.16 mL, 2.0 mmol), and TEA (0.28 mL, 2.0 mmol). Yield: 0.15 g (50%); mp 169−171 °C. ^{1}H NMR (DMSO-d_6) δ 1.10 (6H, br s, 2 × CH$_3$), 1.46 (2H, br s, CH$_2$), 1.63 (4H, br s, 2 × CH$_2$), 1.89−1.92 (2H, m, CH$_2$), 1.97 (2H, br s, CH$_2$), 2.51 (3H, s, CH$_3$), 2.61 (5H, br s, CH and 2 × CH$_2$), 2.87−2.91 (2H, m, CH$_2$), 3.19−3.24 (4H, m, 2 × CH$_2$), 3.74−3.75 (2H, m, CH$_2$), 4.67−4.72 (2H, m, 2NH, exchangeable), 5.27 (2H, s, OCH$_2$), 5.61 (2H, s, OCH$_2$), 7.44−7.46 (1H, m, ArH), 7.51−7.54 (1H, m, ArH), 7.90−7.93 (2H, m, ArH), 8.38 (1H, s, ArH), 8.41 (1H, s, ArH). ^{13}C NMR (CDCl$_3$) δ 9.0, 15.2, 15.3, 24.7, 26.3, 28.1, 35.8, 50.3, 51.4, 57.6, 58.6, 62.7, 109.7, 115.5, 116.4, 119.6, 120.6, 125.7, 126.1, 126.2, 126.6, 127.8, 127.9, 128.9, 130.6, 135.0, 155.1, 156.4, 156.6. HRMS [ESI$^+$]: calcd for $C_{34}H_{44}N_6O_4$, 425.2704 [M + H − 2(OCONHC$_2$H$_5$)]$^+$, found 425.2707.

Cytotoxicity Assay. The cytotoxicity of the newly synthesized hybrid compounds to the human lymphoblastic leukemia cell line CCRF-CEM and its vinblastine-resistant subline CCRF-CEM/VBL; human NSCLC cell lines H460, A549, H520, H226, H2170, H1975, and H1650; human SCLC cell lines H1417, H146, H82, H526, and H211; human colorectal cancer cell line HCT-116; human pancreatic carcinoma cell line Paca S1; and human renal cell adenocarcinoma cell line 786-O were determined by the PrestoBlue (Invitrogen) assay.[34] In general, 3000 cells were plated in 96-well plates 1 day prior to drug treatment. For slow-growing cell lines, such as H1417, H146, and H82, 10 000, 9000, and 5000 cells were plated, respectively. For H211, a fast-growing cell line, 1000 cells were used. The cells were incubated with various compounds at a series of twofold dilutions for 72 h. At the end of incubation, an aliquot of PrestoBlue solution was added, and the cells were further incubated at 37 °C for an additional 1−2 h. The absorbance at 570 and 600 nm was measured using a microplate reader. The dose-effect relationship at six or seven concentrations of each drug was used to determine IC$_{50}$ values using CompuSyn software (version 1.0.1; CompuSyn, Paramus, NJ).[35]

DNA Interstrand Cross-Linking Assay. The formation of DNA ICLs was analyzed by alkaline agarose gel electrophoresis as previously described.[30] In brief, purified pEGFP-N1 plasmid DNA (1.5 μg) was reacted with compounds **19a**, **19b**, **19c**, **19d**, **19e** and melphalan in 40 μL of binding buffer (30 mM sodium chloride/10 mM sodium phosphate, pH 7.4, and 10 mM EDTA) at 37 °C for 2 h. Linearized (by *Bam*H1 digestion) plasmid DNA was then separated by electrophoresis in a 0.8% alkaline agarose gel in NaOH-EDTA buffer at 15 V for 16 h. DNA was visualized under UV light after staining the gels with an ethidium bromide solution.

DNA ICLs formed in nuclear DNA were detected by a modified comet assay.[8] In brief, H562 cells were treated with various concentrations of compound **19a** or cisplatin for 2 h. Afterward, the cells were harvested and irradiated with X-rays at a dose of 20 Gy. An 80 μL aliquot of cell suspension was mixed with 400 μL of 1.2% low-melting-point agarose and plated on a Fisherfinest microscope slide (Thermo Scientific), which was previously layered with 120 μL of 1% agarose gel. Cells were lysed in alkaline buffer (300 mM NaOH and 1 mM EDTA, pH 13.5) prior to electrophoresis. The gels were neutralized before staining with 60 μL of 5 μM YOYO-1 iodide (491/509) (Invitrogen). The tail moment (electrophoretically drawn out fragmented DNA) of 100 cells of each treatment was determined with modified comet assay III software (Perceptive Instruments).

DNA Binding Assay. The binding of compound **19a** to DNA was analyzed by fluorescence titration and DNA melting temperature assay.[40,41] The fluorescence titration was carried out with a Hitachi F-4500 fluorescence spectrophotometer (Jasco, Tokyo, Japan). The cell compartments were thermostated at 25 °C. The fluorescence spectra were obtained from 400 to 480 nm with both excitation and emission slits being 5 nm. The excitation wavelength was 380 nm. Fluorescence titration was carried out by the stepwise addition of an aliquot of TA-rich or CG-rich duplexes (final concentrations from 0.1 to 250 μM) to compound **19a** (5 μM) in 50 μM sodium cacodylate buffer (pH 7.3) containing 5 μM MgCl$_2$. To determine thermal stabilization, the T_m values of the DNA duplexes were analyzed as previously described using a JASCO UV/VIS spectrophotometer by monitoring the sample absorption at 380 nm. CG-rich or TA-rich duplexes (3 μM) interacted with compound **19a** (3 μM) for 2 h in sodium cacodylate buffer containing 5 μM MgCl$_2$. The absorption was then determined by increasing the temperature from 5 to 95 °C at a rate of 0.5 °C/min. The T_m values were determined by the polynomial fitting of the observed curves and were considered to be the temperatures corresponding to the half-dissociation of the DNA duplexes.

Cell Cycle Analysis. The effects of compound **19a** on cell cycle progression were analyzed by flow cytometry as previously described.[62] In brief, ∼2.0 × 10^5 SCLC H526 cells were seeded in each well of a six-well plate and incubated at 37 °C overnight. After treatment with compound **19a** for 24 and 48 h, the suspended cells were centrifuged, fixed in ice-cold 70% ethanol, and kept at −20 °C overnight. The cells were then stained with 4 μg/mL propidium iodide in phosphate-buffered saline (PBS) containing 0.1 mg/mL RNase A and 1% Triton X-100 and then subjected to flow cytometry analysis (FACScan flow cytometer; Becton Dickinson, San Jose, CA). The cell cycle phase distribution was analyzed using FlowJo 7.6 software (Verity Software House, Topsham, ME).

Apoptosis Assay. Apoptotic death was analyzed by Annexin-V staining assay as previously reported.[63] The growing SCLC H526 cells were treated with various concentrations of compound **19a** (0, 0.01, 0.02, 0.04, 0.08 μM) and cisplatin (2, 4, 8, 16) for 72 h. The cells were harvested, and apoptotic cells were detected by flow cytometry using an Annexin-V-FITC Apoptosis Detection Kit (eBiosciences, San Diego, CA) and quantitated by FlowJo 10 software.

Tube Formation Assay. EA.hy926 hybrid endothelial cells were first treated with compound **19a** or **19d** or vatalanib at various concentrations for 24 h. Afterward, the cells were harvested, and an aliquot of cells (8 × 10^3 cells/100 μL/well) was seeded in medium containing 1% FBS on a 96-well plate (ibidi, Munich, Germany), which was precoated with 10 μL of Matrigel (Corning, NY) for 1 h at 37 °C before use. After a 24 h incubation, photos of tube formation were captured under phase contrast microscopy. The nodes of tube formation were determined using Angiogenesis Analyzer from ImageJ. The total number of nodes was averaged by counting the branch points of tube-like structures in three random fields.

Directed *In Vivo* Angiogenesis Assay (DIVAA). The *in vivo* antiangiogenesis activity of compound **19a** was evaluated by DIVAA.[64] A DIVAA Inhibition Kit was obtained from Trevigen (Gaithersburg, MD). The assay protocol was performed according to the manufacturer's instructions. In brief, angioreactors filled with matrix gel containing FGF (37.5 ng)/VEGF (12.5 ng) served as a positive control, whereas angioreactors filled with reduced growth factor BME served as a negative control group. For the experimental groups, the angioreactors contained various concentrations of **19a** (4, 8, and 16 μM) and vatalanib (20, 40, and 80 μM) in BME containing FGF/VEGF, respectively. Three angioreactors were subcutaneously

https://doi.org/10.1021/acs.jmedchem.0c01733
J. Med. Chem. 2021, 64, 12469−12486

implanted into both flanks of nude mice. After 15 days, the angioreactors were excised and labeled with FITC-lectin at 4 °C overnight. The pellets were washed and subjected to fluorescence intensity determination as an indicator of vascular invasion. Data are expressed as mean ± SD. Statistical analyses were performed using Student's *t* test.

Western Blotting Analysis. Phosphorylated VEGFR-2 (p-VEGFR-2) was analyzed by western blotting.[13] In brief, EA.hy926 cells were seeded in a 100 mm dish and treated with various concentrations of compound **19a** or vatalanib for 12 h. The cell lysates were prepared in RIPA lysis buffer with 1% cocktail phosphatase inhibitors on ice. The whole-cell proteins were electrophoretically separated and transferred onto a membrane at 15 V for 12 h. After blocking with 5% milk, the blotted membranes were incubated with anti-VEGFR-2 (Abcam) or anti-p-VEGFR-2 (Abcam) antibody overnight. After washing, the membranes were allowed to react with the secondary anti-rabbit antibody. The proteins were visualized by chemiluminescence using HRP substrate reagent (EMD Millipore).

Therapeutic Efficacy in Animals. All animal studies followed the guidelines approved by the Institutional Animal Care and Use Committee. Male athymic nude mice bearing the nu/nu gene (5 weeks old) were obtained from the National Laboratory Animal Center (Taipei, Taiwan) and housed for 1 week before experimental manipulation. The therapeutic efficacy of **19a** against SCLC H526, renal carcinoma 786-O, and lung squamous H520 xenografts was analyzed following a previous protocol.[13] In brief, an aliquot of H526 (1×10^7 cells), 786-O (0.5×10^7 cells), or H520 (1×107 cells) cells suspended in 100 μL of PBS was subcutaneously implanted into the dorsal flank of each mouse. When the tumor size reached 100−200 mm^3, mice bearing tumors (5 mice for each group) were treated with compound **19a**, cisplatin, or sorafenib. Compound **19a** was given via either i.v. injection or p.o. administration. For i.v. injection, compound **19a** was prepared in a mixture of Tween 80/PEG 400/Kolliphor HS15/ethanol/5% dextrose (5:5:20:30:40, v/v/v/v/v) and administered via the tail vein for 5 consecutive days with a 1-day rest for 2 cycles (QD × 5 + R) × 2. For control group, vehicle was administrated via tail vein. For oral administration, compound **19a** was formulated in a mixture of Tween 80/PEG 400/Kolliphor HS40/ethanol/5% dextrose (2.5:2.5:10:15:70, v/v/v/v/v). The protocol for p.o. treatment was the same as that for i.v. injection. The doses of compound **19a** for i.v. and p.o. were 20 and 60 mg/kg, respectively. Cisplatin, obtained from Across and dissolved in 5% dextrose solution, was i.v. injected at a dose of 4 mg/kg every 4 days three times (Q4D × 3). Sorafenib (Nexavar) tablets were ground into a fine powder, calculated to determine the effective dose, and administered p.o. to mice at 30 or 60 mg/kg for 2 cycles of 5-day treatment with 1-day intervals, the same protocol used for compound **19a**. Control mice were given vehicle using the same protocol as that for compound **19a**. Tumor volume was measured by the aid of a caliper and calculated by the following formula: (length × width^2)/2.

■ ASSOCIATED CONTENT

Supporting Information

The Supporting Information is available free of charge at https://pubs.acs.org/doi/10.1021/acs.jmedchem.0c01733.

Cytotoxicity of compounds **19a** and **19e** to multidrug-resistant KB/vin 10 cells, fetal human colon epithelial cells, and human skin fibroblast; ^{1}H and ^{13}C NMR spectra, EMS-MS spectra, and HPLC chromatograms of intermediates and new compounds (PDF)

Molecular formula strings (CSV)

■ AUTHOR INFORMATION

Corresponding Authors

Tsann-Long Su − *Institute of Biomedical Sciences, Academia Sinica, Taipei 11529, Taiwan*; Email: tlsu@ibms.sinica.edu.tw

Te-Chang Lee − *Institute of Biomedical Sciences, Academia Sinica, Taipei 11529, Taiwan*; orcid.org/0000-0003-4448-1507; Email: bmtcl@ibms.sinica.edu.tw

Authors

Tai-Lin Chen − *Institute of Biomedical Sciences, Academia Sinica, Taipei 11529, Taiwan; School of Pharmacy, China Medical University, Taichung 40400, Taiwan*

Anilkumar S. Patel − *Institute of Biomedical Sciences, Academia Sinica, Taipei 11529, Taiwan; Department of Chemistry, Atmiya University, Rajkot 360005 Gujarat, India*; orcid.org/0000-0002-5232-3421

Vicky Jain − *Institute of Biomedical Sciences, Academia Sinica, Taipei 11529, Taiwan; Department of Chemistry, Marwadi University, Rajkot 360003 Gujarat, India*

Ramajayam Kuppusamy − *Institute of Biomedical Sciences, Academia Sinica, Taipei 11529, Taiwan*

Yi-Wen Lin − *Institute of Biomedical Sciences, Academia Sinica, Taipei 11529, Taiwan*

Ming-Hon Hou − *Institute of Genomics and Bioinformatics, National Chung Hsing University, Taichung 40227, Taiwan*

Complete contact information is available at: https://pubs.acs.org/10.1021/acs.jmedchem.0c01733

Author Contributions

T.-L.C., A.S.P., and V.J. contributed equally. T.-L.S., A.S.P., and V.J. designed and synthesized the benzologue derivatives. A.S.P., V.J., and R.K. performed spectral analysis. Y.-W.L. performed the cytotoxicity assay. T.-L.C. and M.-H.H. designed and performed drug and DNA binding assays. T.-L.C. designed and performed all biological studies. T.-L.C. and V.J. drafted the manuscript. T.-C.L. and T.-L.S. supervised all of the studies. All authors reviewed and approved the final manuscript.

Notes

The authors declare no competing financial interest.

■ ACKNOWLEDGMENTS

This study was supported by grants from the Ministry of Science and Technology, Taiwan (MOST 107-2320-B-001-008, 108-2320-B-001-002, and 109-2320-B-001-026 to T.-C.L. and T.-L.S.) and from China Medical University, Taiwan (CMU108-N-21 to T.-L.C.). The authors thank Ching-Huang Chen (Chemical Lab of IBMS, Academia Sinica) for technical help with the synthesis of the hybrid molecules.

■ ABBREVIATIONS

DCM, dichloromethane; DMAD, dimethyl acetylene dicarboxylate; DMF, dimethylformamide; EGFR, epidermal growth factor receptor; ICLs, interstrand cross-links; i.v., intravenous; HRMS, high-resolution mass spectra; K_d, binding constant; Hz, Hertz; LAH, lithium aluminum hydride; NSCLC, non-small-cell lung cancer; SAR, structure−activity relationship; SCLC, small cell lung cancer; SOD, superoxide dismutase; SS, single strand; TEA, triethylamine; TKI, tyrosine kinase inhibitor; T_m, DNA melting temperature; UV, ultraviolet;

VEGF, vascular endothelial growth factor; VEGFR, vascular endothelial growth factor receptor

REFERENCES

(1) Bérubé, G. An overview of molecular hybrids in drug discovery. *Expert Opin. Drug Discovery* **2016**, *11*, 281−305.

(2) Kucuksayan, E.; Ozben, T. Hybrid compounds as multitarget directed anticancer agents. *Curr. Top. Med. Chem.* **2017**, *17*, 907−918.

(3) Li, F.; Zhao, C.; Wang, L. Molecular-targeted agents combination therapy for cancer: Developments and potentials. *Int. J. Cancer* **2014**, *134*, 1257−1269.

(4) Mokhtari, R. B.; Homayouni, T. S.; Baluch, N.; Morgatskaya, E.; Kumar, S.; Das, B.; Yeger, H. Combination therapy in combating cancer. *Oncotarget* **2017**, *8*, 38022−38043.

(5) Jia, Y.; Wen, X.; Gong, Y.; Wang, X. Current scenario of indole derivatives with potential anti-drug-resistant cancer activity. *Eur. J. Med. Chem.* **2020**, *200*, No. 112359.

(6) Bozorov, K.; Zhao, J.; Aisa, H. A. 1,2,3-triazole-containing hybrids as leads in medicinal chemistry: A recent overview. *Bioorg. Med. Chem.* **2019**, *27*, 3511−3531.

(7) Gao, F.; Zhang, X.; Wang, T.; Xiao, J. Quinolone hybrids and their anti-cancer activities: An overview. *Eur. J. Med. Chem.* **2019**, *165*, 59−79.

(8) Kakadiya, R.; Dong, H.; Lee, P. C.; Kapuriya, N.; Zhang, X.; Chou, T. C.; Lee, T. C.; Kapuriya, K.; Shah, A.; Su, T. L. Potent antitumor bifunctional DNA alkylating agents, synthesis and biological activities of 3a-aza-cyclopenta[a]indenes. *Bioorg. Med. Chem.* **2009**, *17*, 5614−5626.

(9) Chaniyara, R.; Kapuriya, N.; Dong, H.; Lee, P. C.; Suman, S.; Marvania, B.; Chou, T. C.; Lee, T. C.; Kakadiya, R.; Shah, A.; Su, T. L. Novel bifunctional alkylating agents, 5,10-dihydropyrrolo[1,2-b]isoquinoline derivatives, synthesis and biological activity. *Bioorg. Med. Chem.* **2011**, *19*, 275−286.

(10) Chaniyara, R.; Tala, S.; Chen, C. W.; Lee, P. C.; Kakadiya, R.; Dong, H.; Marvania, B.; Chen, C. H.; Chou, T. C.; Lee, T. C.; Shah, A.; Su, T. L. Synthesis and antitumor evaluation of novel benzo[d]pyrrolo[2,1-b]thiazole derivatives. *Eur. J. Med. Chem.* **2012**, *53*, 28−40.

(11) Chaniyara, R.; Tala, S.; Chen, C. W.; Zang, X.; Kakadiya, R.; Lin, L. F.; Chen, C. H.; Chien, S. I.; Chou, T. C.; Tsai, T. H.; Lee, T. C.; Shah, A.; Su, T. L. Novel antitumor indolizino[6,7-b]indoles with multiple modes of action: DNA cross-linking and topoisomerase i and ii inhibition. *J. Med. Chem.* **2013**, *56*, 1544−1563.

(12) Chen, C. W.; Wu, M. H.; Chen, Y. F.; Yen, T. Y.; Lin, Y. W.; Chao, S. H.; Tala, S.; Tsai, T. H.; Su, T. L.; Lee, T. C. A potent derivative of indolizino[6,7-b]indole for treatment of human non-small cell lung cancer cells. *Neoplasia* **2016**, *18*, 199−212.

(13) Chang, S. M.; Jain, V.; Chen, T. L.; Patel, A. S.; Pidugu, H. B.; Lin, Y. W.; Wu, M. H.; Huang, J. R.; Wu, H. C.; Shah, A.; Su, T. L.; Lee, T. C. Design and synthesis of 1,2-bis(hydroxymethyl)pyrrolo-[2,1- a]phthalazine hybrids as potent anticancer agents that inhibit angiogenesis and induce DNA interstrand cross-links. *J. Med. Chem.* **2019**, *62*, 2404−2418.

(14) Anderson, W. K.; Corey, P. F. Synthesis and antileukemic activity of 5-substituted 2,3-dihydro-6,7-bis(hydroxymethyl)-1h-pyrrolizine diesters. *J. Med. Chem.* **1977**, *20*, 812−818.

(15) Sangshetti, J.; Pathan, S. K.; Patil, R.; Akber Ansari, S.; Chhajed, S.; Arote, R.; Shinde, D. B. Synthesis and biological activity of structurally diverse phthalazine derivatives: A systematic review. *Bioorg. Med. Chem.* **2019**, *27*, 3979−3997.

(16) Vila, N.; Besada, P.; Costas, T.; Costas-Lago, M. C.; Teran, C. Phthalazin-1(2h)-one as a remarkable scaffold in drug discovery. *Eur. J. Med. Chem.* **2015**, *97*, 462−482.

(17) El-Helby, A.-G. A.; Ayyad, R. R. A.; Sakr, H.; El-Adl, K.; Ali, M. M.; Khedr, F. Design, synthesis, molecular docking, and anticancer activity of phthalazine derivatives as vegfr-2 inhibitors. *Arch. Pharm.* **2017**, *350*, No. 1700240.

(18) Abou-Seri, S. M.; Eldehna, W. M.; Ali, M. M.; Abou El Ella, D. A. 1-piperazinylphthalazines as potential vegfr-2 inhibitors and anticancer agents: Synthesis and in vitro biological evaluation. *Eur. J. Med. Chem.* **2016**, *107*, 165−179.

(19) Amin, K. M.; Barsoum, F. F.; Awadallah, F. M.; Mohamed, N. E. Identification of new potent phthalazine derivatives with vegfr-2 and egfr kinase inhibitory activity. *Eur. J. Med. Chem.* **2016**, *123*, 191−201.

(20) Bold, G.; Altmann, K. H.; Frei, J.; Lang, M.; Manley, P. W.; Traxler, P.; Wietfeld, B.; Bruggen, J.; Buchdunger, E.; Cozens, R.; Ferrari, S.; Furet, P.; Hofmann, F.; Martiny-Baron, G.; Mestan, J.; Rosel, J.; Sills, M.; Stover, D.; Acemoglu, F.; Boss, E.; Emmenegger, R.; Lasser, L.; Masso, E.; Roth, R.; Schlachter, C.; Vetterli, W.; et al. New anilinophthalazines as potent and orally well absorbed inhibitors of the vegf receptor tyrosine kinases useful as antagonists of tumor-driven angiogenesis. *J. Med. Chem.* **2000**, *43*, 2310−2323.

(21) Wood, J. M.; Bold, G.; Buchdunger, E.; Cozens, R.; Ferrari, S.; Frei, J.; Hofmann, F.; Mestan, J.; Mett, H.; O'Reilly, T.; Persohn, E.; Rosel, J.; Schnell, C.; Stover, D.; Theuer, A.; Towbin, H.; Wenger, F.; Woods-Cook, K.; Menrad, A.; Siemeister, G.; Schirner, M.; Thierauch, K. H.; Schneider, M. R.; Drevs, J.; Martiny-Baron, G.; Totzke, F. Ptk787/zk 222584, a novel and potent inhibitor of vascular endothelial growth factor receptor tyrosine kinases, impairs vascular endothelial growth factor-induced responses and tumor growth after oral administration. *Cancer Res.* **2000**, *60*, 2178−2189.

(22) Duncton, M. A.; Piatnitski Chekler, E. L.; Katoch-Rouse, R.; Sherman, D.; Wong, W. C.; Smith, L. M., 2nd; Kawakami, J. K.; Kiselyov, A. S.; Milligan, D. L.; Balagtas, C.; Hadari, Y. R.; Wang, Y.; Patel, S. N.; Rolster, R. L.; Tonra, J. R.; Surguladze, D.; Mitelman, S.; Kussie, P.; Bohlen, P.; Doody, J. F. Arylphthalazines as potent, and orally bioavailable inhibitors of vegfr-2. *Bioorg. Med. Chem.* **2009**, *17*, 731−740.

(23) Eldehna, W. M.; Abou-Seri, S. M.; El Kerdawy, A. M.; Ayyad, R. R.; Hamdy, A. M.; Ghabbour, H. A.; Ali, M. M.; Abou El Ella, D. A. Increasing the binding affinity of vegfr-2 inhibitors by extending their hydrophobic interaction with the active site: Design, synthesis and biological evaluation of 1-substituted-4-(4-methoxybenzyl)-phthalazine derivatives. *Eur. J. Med. Chem.* **2016**, *113*, 50−62.

(24) Su, T. L.; Lee, T. C.; Kakadiya, R. The development of bis(hydroxymethyl)pyrrole analogs as bifunctional DNA cross-linking agents and their chemotherapeutic potential. *Eur. J. Med. Chem.* **2013**, *69*, 609−621.

(25) Cheshire, D. R. How well do medicinal chemists learn from experience? *Drug Discovery Today* **2011**, *16*, 817−821.

(26) Pedreira, J. G. B.; Franco, L. S.; Barreiro, E. J. Chemical intuition in drug design and discovery. *Curr. Top. Med. Chem.* **2019**, *19*, 1679−1693.

(27) Keri, R. S.; Chand, K.; Budagumpi, S.; Balappa Somappa, S.; Patil, S. A.; Nagaraja, B. M. An overview of benzo[b]thiophene-based medicinal chemistry. *Eur. J. Med. Chem.* **2017**, *138*, 1002−1033.

(28) Malgorzata, J.; Suwinska, K.; Besnard, C.; Pluta, K.; Morak-Mlodawska, B. The structures of 8- and 10-trifluoromethylquino[3,2-b]benzo[1,4]thianzines and their benzyl derivatives. *Heterocycles* **2012**, *85*, 2281−2290.

(29) Shan, Y. Y.; Zhang, C. M.; Tang, L. Q.; Liu, Z. P.; Bearss, N. R.; Sarver, J. G.; Luniwal, A.; Erhardt, P. W. Syntheses of 2,3-diarylated 2h-benzo[e][1,2]thiazine 1,1-dioxides and their 3,4-dihydro derivatives, and assessment of their inhibitory activity against mcf-7 breast cancer cells. *Med. Chem.* **2011**, *7*, 561−571.

(30) Sánchez-Moreno, M.; Sanz, A. M.; Gomez-Contreras, F.; Navarro, P.; Marin, C.; Ramirez-Macias, I.; Rosales, M. J.; Olmo, F.; Garcia-Aranda, I.; Campayo, L.; Cano, C.; Arrebola, F.; Yunta, M. J. In vivo trypanosomicidal activity of imidazole- or pyrazole-based benzo[g]phthalazine derivatives against acute and chronic phases of chagas disease. *J. Med. Chem.* **2011**, *54*, 970−979.

(31) Sánchez-Moreno, M.; Gomez-Contreras, F.; Navarro, P.; Marin, C.; Ramirez-Macias, I.; Rosales, M. J.; Campayo, L.; Cano, C.; Sanz, A. M.; Yunta, M. J. Imidazole-containing phthalazine derivatives inhibit fe-sod performance in leishmania species and are active in vitro against visceral and mucosal leishmaniasis. *Parasitology* **2015**, *142*, 1115−1129.

https://doi.org/10.1021/acs.jmedchem.0c01733
J. Med. Chem. 2021, 64, 12469−12486

(32) Costes, N.; Le Deit, H.; Michel, S.; Tillequin, F.; Koch, M.; Pfeiffer, B.; Renard, P.; Leonce, S.; Guilbaud, N.; Kraus-Berthier, L.; Pierre, A.; Atassi, G. Synthesis and cytotoxic and antitumor activity of benzo[b]pyrano[3, 2-h]acridin-7-one analogues of acronycine. *J. Med. Chem.* **2000**, *43*, 2395−2402.
(33) David-Cordonnier, M. H.; Laine, W.; Lansiaux, A.; Kouach, M.; Briand, G.; Pierre, A.; Hickman, J. A.; Bailly, C. Alkylation of guanine in DNA by s23906-1, a novel potent antitumor compound derived from the plant alkaloid acronycine. *Biochemistry* **2002**, *41*, 9911−9920.
(34) Pons, M.; Campayo, L.; Martinez-Balbas, M. A.; Azorin, F.; Navarro, P.; Giralt, E. A new ionizable chromophore of 1,4-bis(alkylamino)benzo[g]phthalazine which interacts with DNA by intercalation. *J. Med. Chem.* **1991**, *34*, 82−86.
(35) Gandolfi, C. A.; Beggiolin, G.; Menta, E.; Palumbo, M.; Sissi, C.; Spinelli, S.; Johnson, F. Chromophore-modified antitumor anthracenediones: Synthesis, DNA binding, and cytotoxic activity of 1,4-bis[(aminoalkyl)amino]benzo[g]-phthalazine-5,10-diones. *J. Med. Chem.* **1995**, *38*, 526−536.
(36) Pérez, C.; Campayo, L.; Navarro, P.; Garcia-Bermejo, L.; Aller, P. The action of the DNA intercalating agents 4′-(9-acridinylamino) methanesulphon-m-anisidide and 1,4-bis(butylamino) benzo[g]-phthalazine in u-937 human promonocytic cells: Relationship between cell cycle and differentiation. *Biochem. Pharmacol.* **1994**, *48*, 75−82.
(37) Anderson, W. K.; New, J. S.; Corey, P. F. Vinylogous carbinolamine tumor inhibitors. 7. Tumor inhibitory agents: Bis-(n-alkylcarbamate) derivatives of 2,3-dihydro-5-(3′,4′-dichlorophenyl)-6,7-bis(hydroxymethyl)-1h-pyrrolizine. *Arzneimittelforschung* **1980**, *30*, 765−767.
(38) Lee, P. C.; Kakadiya, R.; Su, T. L.; Lee, T. C. Combination of bifunctional alkylating agent and arsenic trioxide synergistically suppresses the growth of drug-resistant tumor cells. *Neoplasia* **2010**, *12*, 376−387.
(39) Hartley, J. A.; Berardini, M. D.; Souhami, R. L. An agarose gel method for the determination of DNA interstrand crosslinking applicable to the measurement of the rate of total and "second-arm" crosslink reactions. *Anal. Biochem.* **1991**, *193*, 131−134.
(40) Chien, C. M.; Wu, P. C.; Satange, R.; Chang, C. C.; Lai, Z. L.; Hagler, L.; Zimmerman, S. C.; Hou, M. H. Structural basis for targeting t:T mismatch with triaminotriazine-acridine conjugate induces a u-shaped head-to-head four-way junction in ctg repeat DNA. *J. Am. Chem. Soc.* **2020**, *142*, 11165−11172.
(41) Lo, Y. S.; Lin, S. Y.; Wang, S. M.; Wang, C. T.; Chiu, Y. L.; Huang, T. H.; Hou, M. H. Oligomerization of the carboxyl terminal domain of the human coronavirus 229e nucleocapsid protein. *FEBS Lett.* **2013**, *587*, 120−127.
(42) Woo, J. S.; Sigurdsson, S. T.; Hopkins, P. B. DNA interstrand cross-linking reactions of pyrrole-derived, bifunctional electrophiles - evidence for a common target site in DNA. *J. Am. Chem. Soc.* **1993**, *115*, 3407−3415.
(43) Bergers, G.; Hanahan, D. Modes of resistance to anti-angiogenic therapy. *Nat. Rev. Cancer* **2008**, *8*, 592−603.
(44) Yadav, L.; Puri, N.; Rastogi, V.; Satpute, P.; Sharma, V. Tumour angiogenesis and angiogenic inhibitors: A review. *J. Clin. Diagn. Res.* **2015**, *9*, XE01−XE05.
(45) Loizzi, V.; Del Vecchio, V.; Gargano, G.; De Liso, M.; Kardashi, A.; Naglieri, E.; Resta, L.; Cicinelli, E.; Cormio, G. Biological pathways involved in tumor angiogenesis and bevacizumab based anti-angiogenic therapy with special references to ovarian cancer. *Int. J. Mol. Sci.* **2017**, *18*, No. 1967.
(46) Roskoski, R., Jr. Vascular endothelial growth factor (vegf) signaling in tumor progression. *Crit. Rev. Oncol. Hematol.* **2007**, *62*, 179−213.
(47) Ferrara, N.; Kerbel, R. S. Angiogenesis as a therapeutic target. *Nature* **2005**, *438*, 967−974.
(48) Burnette, W. N. "Western blotting": Electrophoretic transfer of proteins from sodium dodecyl sulfate−polyacrylamide gels to unmodified nitrocellulose and radiographic detection with antibody and radioiodinated protein a. *Anal. Biochem.* **1981**, *112*, 195−203.
(49) Senger, D. R.; Perruzzi, C. A.; Streit, M.; Koteliansky, V. E.; de Fougerolles, A. R.; Detmar, M. The alpha(1)beta(1) and alpha(2)-beta(1) integrins provide critical support for vascular endothelial growth factor signaling, endothelial cell migration, and tumor angiogenesis. *Am. J. Pathol.* **2002**, *160*, 195−204.
(50) Sastry, S. V.; Nyshadham, J. R.; Fix, J. A. Recent technological advances in oral drug delivery - a review. *Pharm. Sci. Technol. Today* **2000**, *3*, 138−145.
(51) Fossella, F.; Pereira, J. R.; von Pawel, J.; Pluzanska, A.; Gorbounova, V.; Kaukel, E.; Mattson, K. V.; Ramlau, R.; Szczesna, A.; Fidias, P.; Millward, M.; Belani, C. P. Randomized, multinational, phase iii study of docetaxel plus platinum combinations versus vinorelbine plus cisplatin for advanced non-small-cell lung cancer: The tax 326 study group. *J. Clin. Oncol.* **2003**, *21*, 3016−3024.
(52) Cataldo, V. D.; Gibbons, D. L.; Perez-Soler, R.; Quintas-Cardama, A. Treatment of non-small-cell lung cancer with erlotinib or gefitinib. *N. Engl. J. Med.* **2011**, *364*, 947−955.
(53) Herbst, R. S.; Soria, J. C.; Kowanetz, M.; Fine, G. D.; Hamid, O.; Gordon, M. S.; Sosman, J. A.; McDermott, D. F.; Powderly, J. D.; Gettinger, S. N.; Kohrt, H. E.; Horn, L.; Lawrence, D. P.; Rost, S.; Leabman, M.; Xiao, Y.; Mokatrin, A.; Koeppen, H.; Hegde, P. S.; Mellman, I.; Chen, D. S.; Hodi, F. S. Predictive correlates of response to the anti-pd-l1 antibody mpdl3280a in cancer patients. *Nature* **2014**, *515*, 563−567.
(54) Sgambato, A.; Casaluce, F.; Sacco, P. C.; Palazzolo, G.; Maione, P.; Rossi, A.; Ciardiello, F.; Gridelli, C. Anti pd-1 and pdl-1 immunotherapy in the treatment of advanced non- small cell lung cancer (nsclc): A review on toxicity profile and its management. *Curr. Drug Saf.* **2016**, *11*, 62−68.
(55) Lopez, A.; Harada, K.; Vasilakopoulou, M.; Shanbhag, N.; Ajani, J. A. Targeting angiogenesis in colorectal carcinoma. *Drugs* **2019**, *79*, 63−74.
(56) Zhao, D.; Hou, H.; Zhang, X. Progress in the treatment of solid tumors with apatinib: A systematic review. *Onco Targets Ther.* **2018**, *11*, 4137−4147.
(57) Vasudev, N. S.; Reynolds, A. R. Anti-angiogenic therapy for cancer: Current progress, unresolved questions and future directions. *Angiogenesis* **2014**, *17*, 471−494.
(58) Tomasello, G.; Petrelli, F.; Ghidini, M.; Russo, A.; Passalacqua, R.; Barni, S. Folfoxiri plus bevacizumab as conversion therapy for patients with initially unresectable metastatic colorectal cancer: A systematic review and pooled analysis. *JAMA Oncol.* **2017**, *3*, No. e170278.
(59) Garcia, J.; Hurwitz, H. I.; Sandler, A. B.; Miles, D.; Coleman, R. L.; Deurloo, R.; Chinot, O. L. Bevacizumab (avastin(r)) in cancer treatment: A review of 15 years of clinical experience and future outlook. *Cancer Treat. Rev.* **2020**, *86*, No. 102017.
(60) Rajora, A. K.; Ravishankar, D.; Zhang, H.; Rosenholm, J. M. Recent advances and impact of chemotherapeutic and antiangiogenic nanoformulations for combination cancer therapy. *Pharmaceutics* **2020**, *12*, No. 592.
(61) Rawal, S.; Patel, M. M. Threatening cancer with nanoparticle aided combination oncotherapy. *J. Controlled Release* **2019**, *301*, 76−109.
(62) Marvania, B.; Kakadiya, R.; Christian, W.; Chen, T. L.; Wu, M. H.; Suman, S.; Tala, K.; Lee, T. C.; Shah, A.; Su, T. L. The synthesis and biological evaluation of new DNA-directed alkylating agents, phenyl n-mustard-4-anilinoquinoline conjugates containing a urea linker. *Eur. J. Med. Chem.* **2014**, *83*, 695−708.
(63) Chen, T. L.; Lin, Y. W.; Chen, Y. B.; Lin, J. J.; Su, T. L.; Shen, C. N.; Lee, T. C. A low-toxicity DNA-alkylating n-mustard-quinoline conjugate with preferential sequence specificity exerts potent antitumor activity against colorectal cancer. *Neoplasia* **2018**, *20*, 119−130.
(64) Guedez, L.; Rivera, A. M.; Salloum, R.; Miller, M. L.; Diegmueller, J. J.; Bungay, P. M.; Stetler-Stevenson, W. G.

https://doi.org/10.1021/acs.jmedchem.0c01733
J. Med. Chem. 2021, 64, 12469−12486

Quantitative assessment of angiogenic responses by the directed in vivo angiogenesis assay. *Am. J. Pathol.* **2003**, *162*, 1431−1439.

https://doi.org/10.1021/acs.jmedchem.0c01733
J. Med. Chem. 2021, 64, 12469−12486